

Collins-Soper kernel with lattice QCD

Artur Avkhadiev¹

in collaboration with

Yang Fu¹, Phiala Shanahan¹, Michael Wagman², and Yong Zhao³

PRD 108 (2023) 11, 114505 [2307.12359]

PRL 132 (2024) 23, 231901 [2402.06725]

+ ongoing work



Massachusetts
Institute of
Technology



Meeting on Lattice Parton Physics from Large Momentum Effective Theory (LaMET)

University of Maryland, College Park

August 11-14, 2024

The Collins-Soper (CS) kernel

- Related to TMDs (transverse-momentum-dependent distributions): a generalization of e.g. PDFs:

$$\text{PDFs } f_{q/h}(x, \mu) \longrightarrow \text{TMD PDFs } f_{q/h}(x, b_T, \mu, \zeta)$$

- Describes RG evolution of TMDs along ζ :

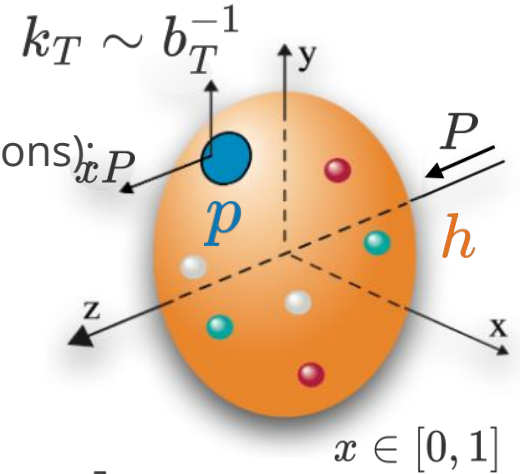
$$f_{p/h}(x, b_T, \mu, \zeta) = f_{p/h}(x, b_T, \mu, \zeta_0) \exp \left[\frac{1}{2} \gamma_p(b_T, \mu) \ln \frac{\zeta}{\zeta_0} \right]$$

- \Rightarrow Computed as a ratio of TMDs at different ζ :

- Independent of hadronic state
- Different for $p \in \{q, g\}$
- Non-perturbative at large b_T (for any μ)

$$\gamma_q(b_T, \mu) = \frac{2}{\ln(\zeta_1/\zeta_2)} \ln \frac{f_{q/h}(x, b_T, \mu, \zeta_1)}{f_{q/h}(x, b_T, \mu, \zeta_2)}$$

Proportional to hadron momentum P



Based on Fig. 1.1 in TMD Handbook, 2304.03302

- Encoded by light-like matrix elements
- Matched onto space-like matrix elements with LaMET \Rightarrow **computable in LQCD**

CS kernel: pheno. models and input from LQCD

Pheno. models fit to experimental data (SIDIS, DY)

$$-\frac{1}{2} \gamma_q^{\text{param.}}(b_T, \mu; B_{\text{NP}}, \{c_i\}) \text{ free parameters}$$

$$= \mathcal{D}_{\text{pert.}}(b^*, \mu) + \mathcal{D}_{\text{NP}}(b_T, b^*; B_{\text{NP}}, \{c_i\})$$

Perturbative term

controlled by $b^*(b_T; B_{\text{NP}})$

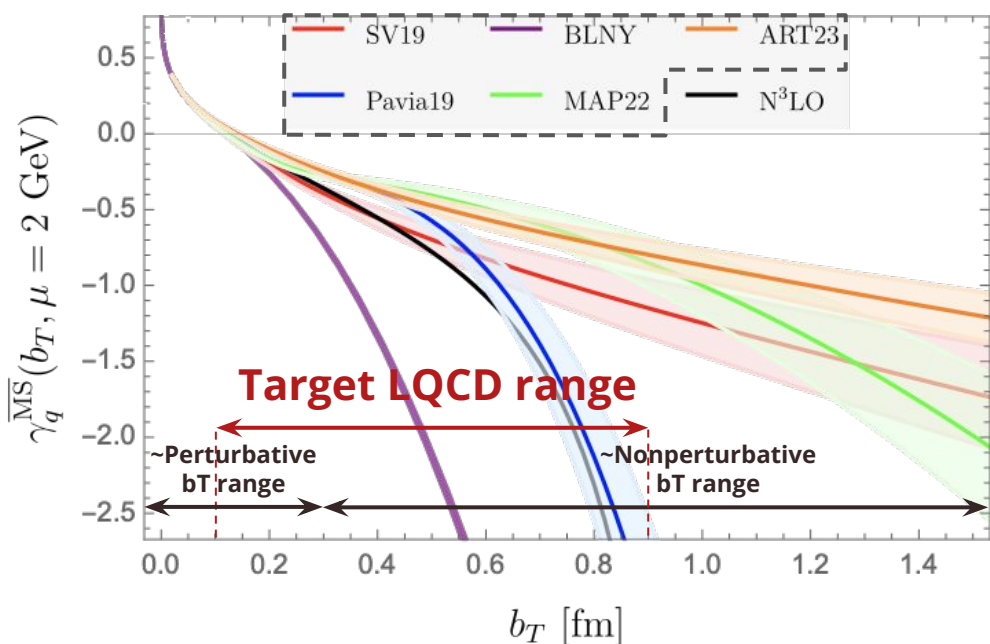
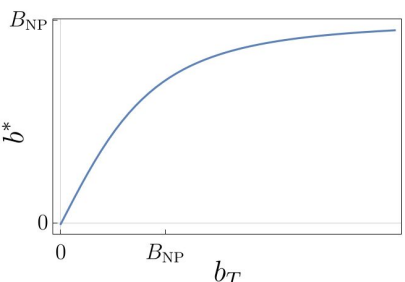
Non-perturbative term

modeled b_T dependence, e.g.

$$\mathcal{D}_{\text{NP}}(b_T, b^*; B_{\text{NP}}, \{c_i\}) = b_T b^* \left[c_0 + c_1 \ln \frac{b^*}{B_{\text{NP}}} \right]$$

or

$$\mathcal{D}_{\text{NP}}(b_T; g_2) = -g_2 \frac{b_T^2}{2}$$



LQCD goal:
sufficient
precision for
direct comparison

BLNY: PRD 67 (2003), [hep-ph/0212159]
SV19: JHEP 06, 137 [1912.06532]
Pavia19: JHEP 07, 117, [1912.07550]
MAP22: JHEP 10, 127, [2206.07598]
ART23: [2305.07473]

Other recent results (not plotted):
Isaacson, Fu, Yuan [2311.09916]
Bury et. al JHEP 10, 118 (2022) [2201.07114]
MAP24 [2405.13833]

LQCD results directly comparable with pheno. models

Fit CS parameterization to \oplus **LQCD data** from 3 lattice spacings

pheno. parameters

$$-\frac{1}{2} \left(\gamma_q^{\text{param.}}(b_T, \mu; B_{\text{NP}}, \{c_i\}) - k_1 \frac{a}{b_T} - k_2 \frac{a^2}{b_T^2} \right)$$

$$= \mathcal{D}_{\text{pert.}}(b^*, \mu) + \mathcal{D}_{\text{NP}}(b_T, b^*; B_{\text{NP}}, \{c_i\})$$

discretization effects

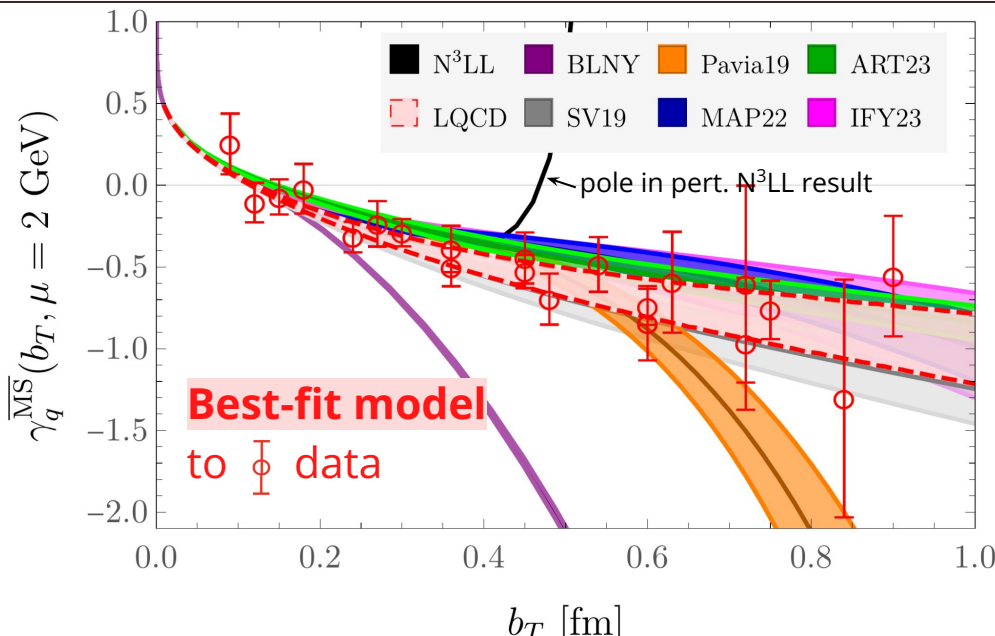
Consistent with:

SV19: JHEP 06, 137, [1912.06532]

MAP22: JHEP 10, 127, [2206.07598]

ART23: [2305.07473]

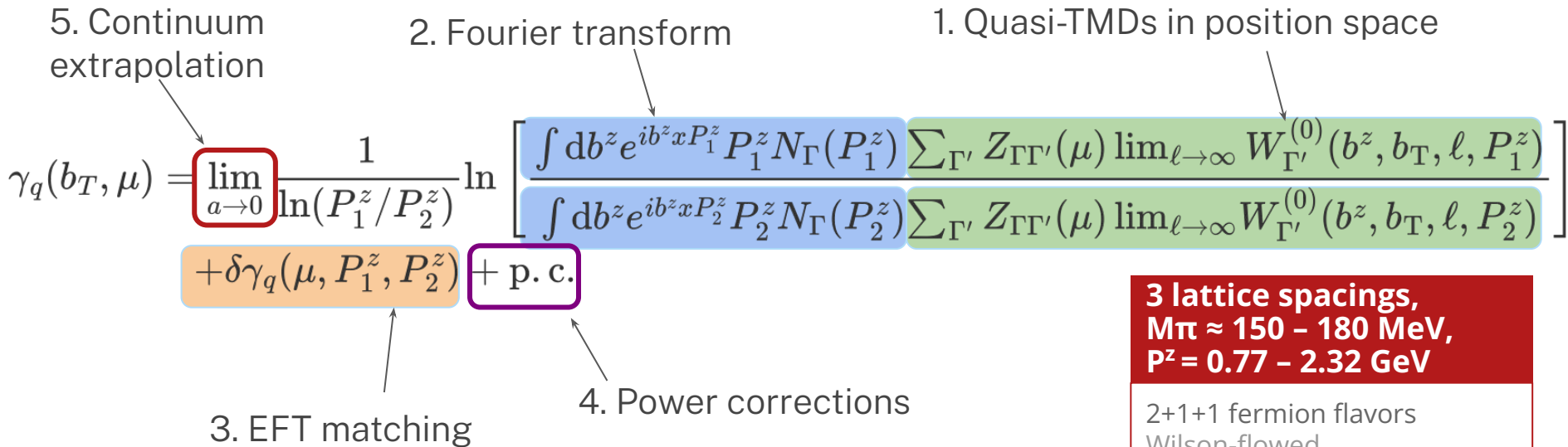
IFY23: Isaacson, Fu, Yuan [2311.09916]



Disfavors at large b_T :
BLNY: PRD 67 (2003), [hep-ph/0212159]
Pavia19: JHEP 07, 117, [1912.07550]

CS kernel from LQCD: outline

X. Ji et. al., Phys. Lett. B 811 [1911.03840]



X. Ji et. al, PRD91 (2015);
Ebert et. al, PRD99 (2019), JHEP09 (2019) 037;

**3 lattice spacings,
M π \approx 150 - 180 MeV,
P z = 0.77 - 2.32 GeV**

2+1+1 fermion flavors
Wilson-flowed
Clover-on-HISQ fermions,

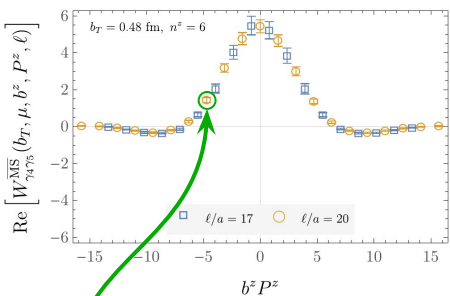
(1) 48 3 x 64, a=0.12 fm,

new: (2) 32 3 x 48, a=0.15 fm

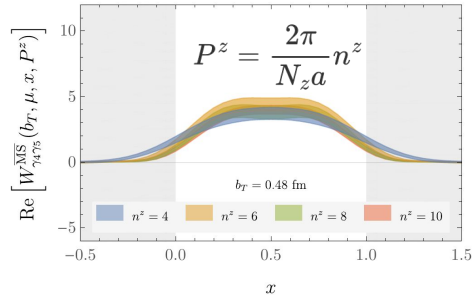
(3) 64 3 x 96, a=0.09 fm

CS kernel from LQCD: outline

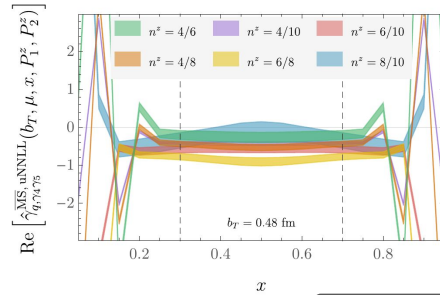
Calculate position-space MEs



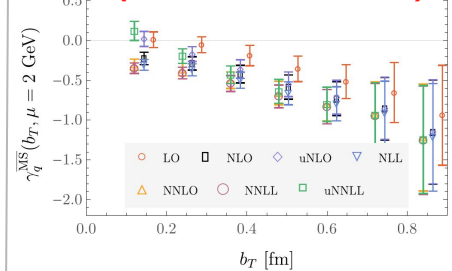
Fourier transform (FT) to momentum-space MEs



Form ratios of MEs + match + fit in x



...repeat for each bT (... and for each a)



$$\sum_{\Gamma'} Z_{\Gamma\Gamma'}(\mu) \lim_{\ell \rightarrow \infty} W_O^{\Gamma'}(b^z, b_T, \ell, P_1^z)$$

$$\int db^z e^{ib^z x P_1^z} P_1^z N_{\Gamma}(P_1^z)$$

$$\sum_{\Gamma'} Z_{\Gamma\Gamma'}(\mu) \lim_{\ell \rightarrow \infty} W_O^{\Gamma'}(b^z, b_T, \ell, P_1^z)$$

$$\gamma_q(b_T, \mu) = \lim_{a \rightarrow 0} \frac{1}{\ln(P_1^z/P_2^z)} \ln \left[\frac{\int db^z e^{ib^z x P_1^z} P_1^z N_{\Gamma}(P_1^z) \sum_{\Gamma'} Z_{\Gamma\Gamma'}(\mu) \lim_{\ell \rightarrow \infty} W_O^{\Gamma'}(b^z, b_T, \ell, P_1^z)}{\int db^z e^{ib^z x P_2^z} P_2^z N_{\Gamma}(P_1^z) \sum_{\Gamma'} Z_{\Gamma\Gamma'}(\mu) \lim_{\ell \rightarrow \infty} W_O^{\Gamma'}(b^z, b_T, \ell, P_2^z)} \right] + \delta\gamma_q(\mu, P_1^z, P_2^z) + \text{p. c.}$$

Each point is a separate matrix element calculation

Position-space quasi-TMDs

- Compute **quasi-TMD wavefunctions (WFs)**

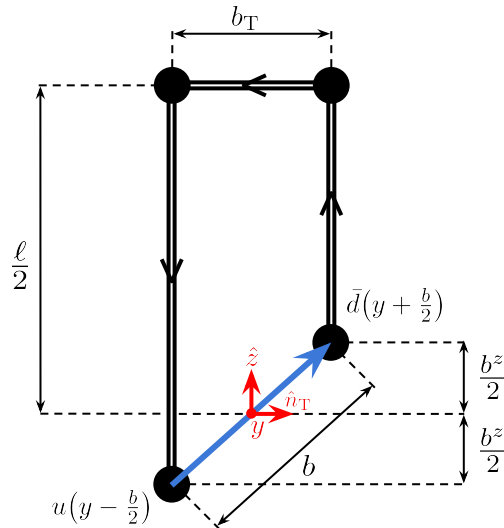
$$\begin{aligned} \phi_{\Gamma}(b_T, b^z, P^z, \ell) \\ = \langle 0 | \mathcal{O}_{\Gamma}(b_T, b^z, 0, \ell) | \pi(P^z) \rangle \end{aligned}$$

- Operators

$$\mathcal{O}_{\Gamma}(b_T, b^z, y, \ell)$$

with staple-shaped Wilson lines

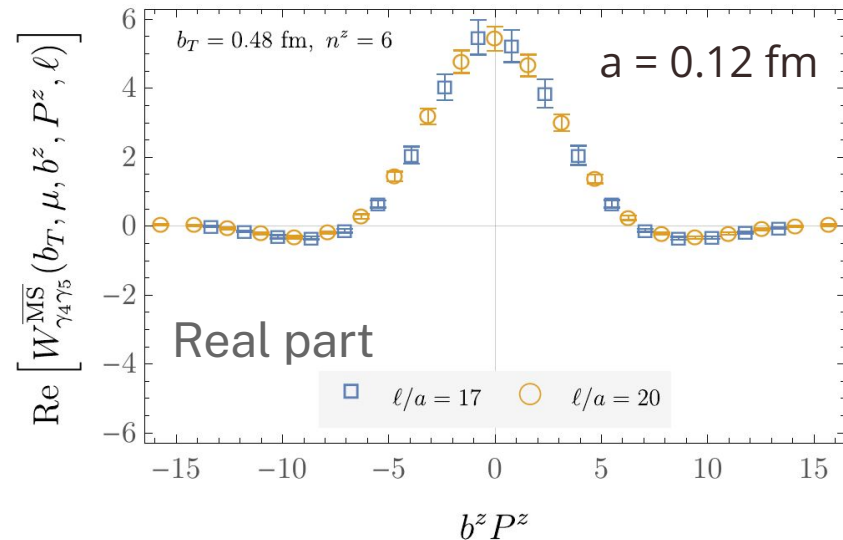
- Separately for each $\mathbf{b}^z, \mathbf{P}^z, \mathbf{b}_T, \ell$, Dirac (Γ) structure



- Matrix elements have divergences $\sim \ell + b_T$

- Subtract divergences in **quasi-TMD WF ratios**

$$W_{\Gamma}^{(0)}(b_T, b^z, P^z, \ell) = \frac{\tilde{\phi}_{\Gamma}(b_T, b^z, P^z, \ell)}{\tilde{\phi}_{\gamma^4 \gamma^5}(b_T, 0, 0, \ell)}$$



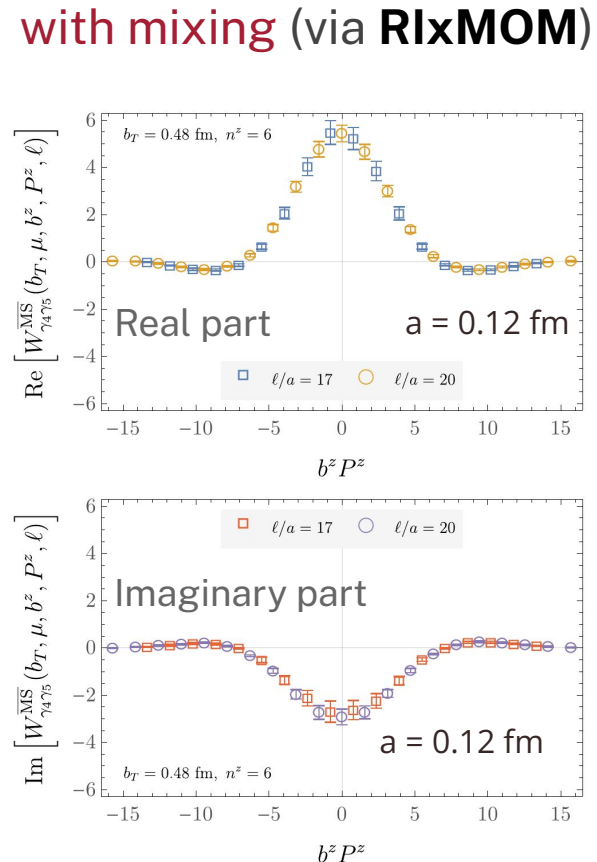
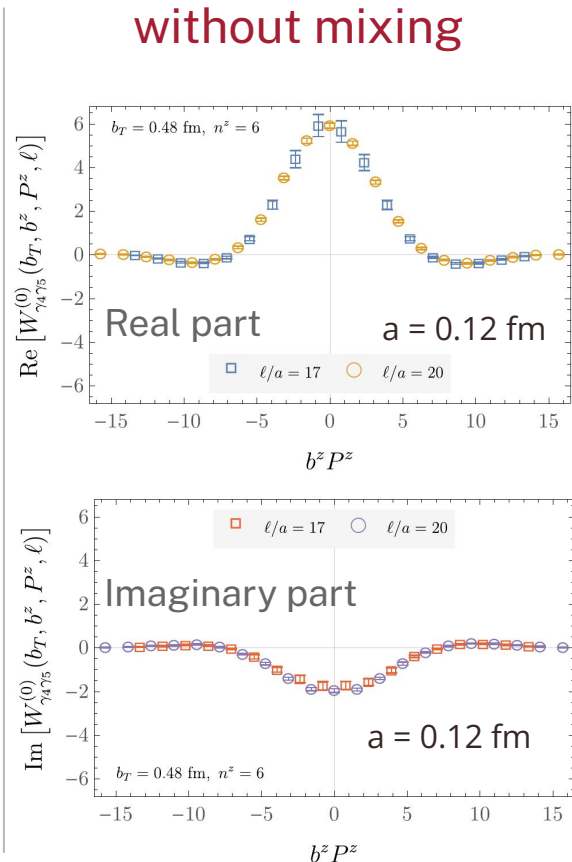
Position-space quasi-TMD WFs

- **Mixing effects** included via **RlxMOM** scheme

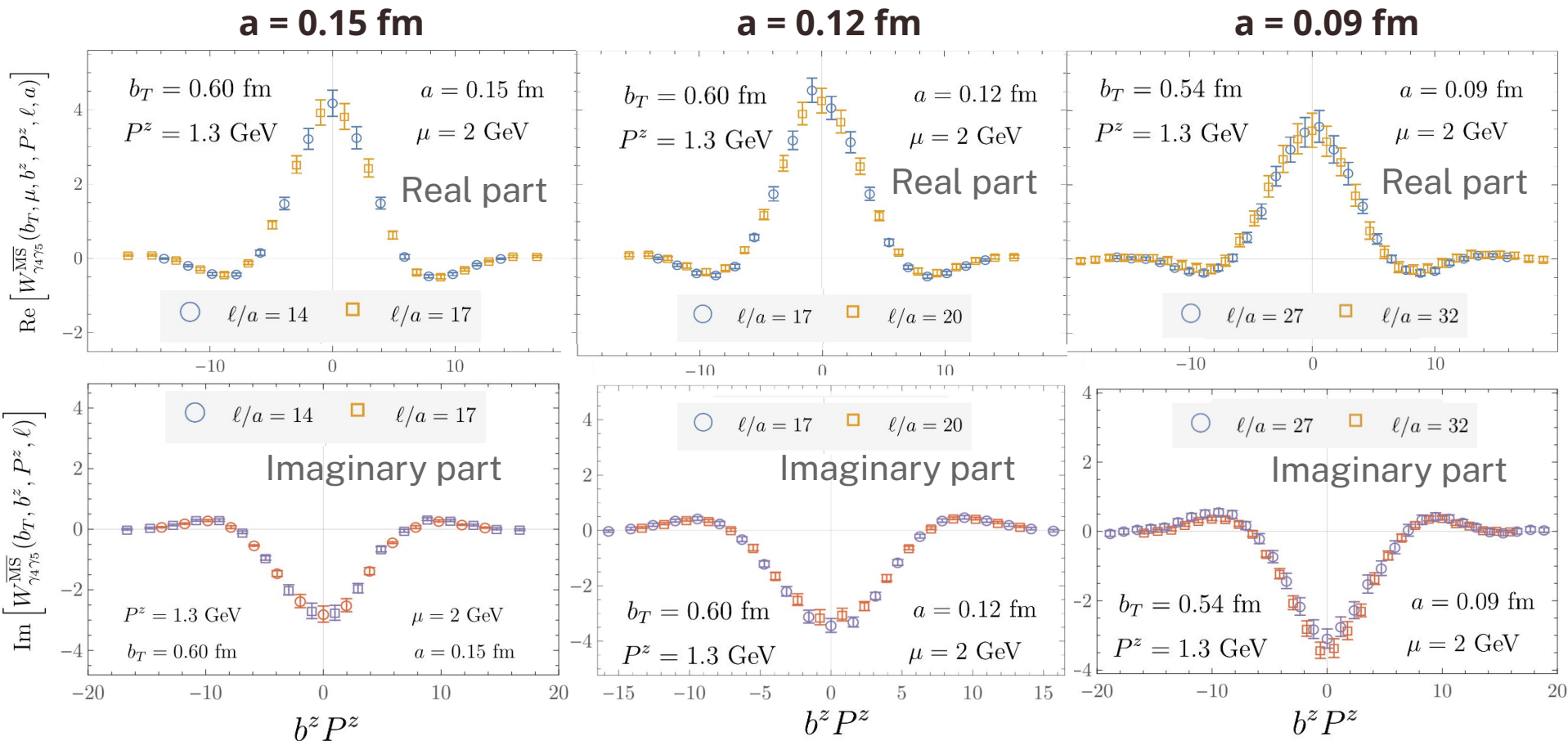
$$W_{\Gamma}^{\overline{\text{MS}}}(b_T, \mu, b^z, P^z, \ell) = \sum_{\Gamma'} Z_{\Gamma\Gamma'}^{\overline{\text{MS}}}(\mu) W_{\Gamma}^{(0)}(b_T, b^z, P^z, \ell)$$

$$\Gamma \in \{\gamma_4\gamma_5, \gamma_3\gamma_5\}$$

- Shown for $b_T = 0.48$ fm, $P_z = 1.29$ GeV
- Consistent between different staple lengths ℓ
- Decay to zero within computed b_z ranges.

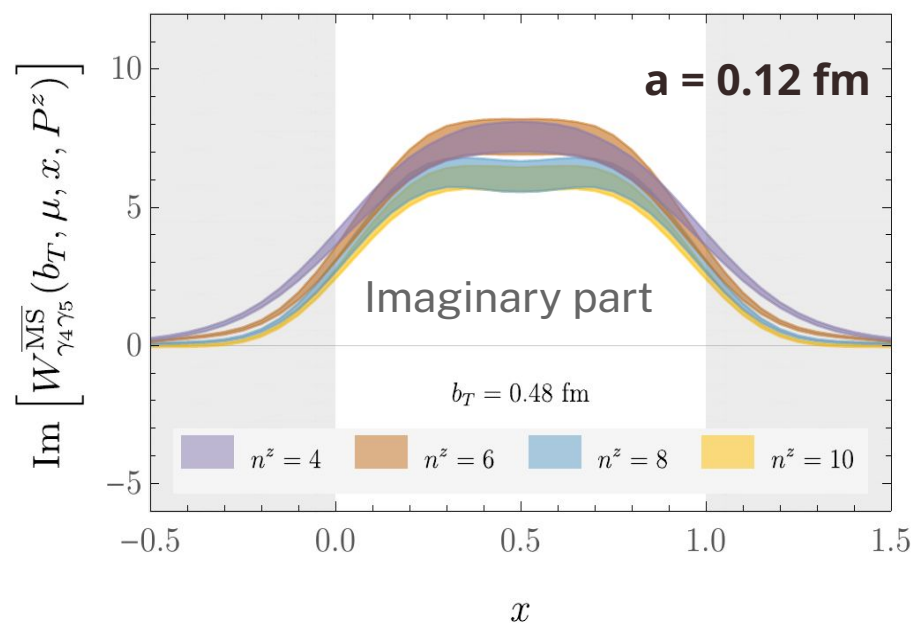
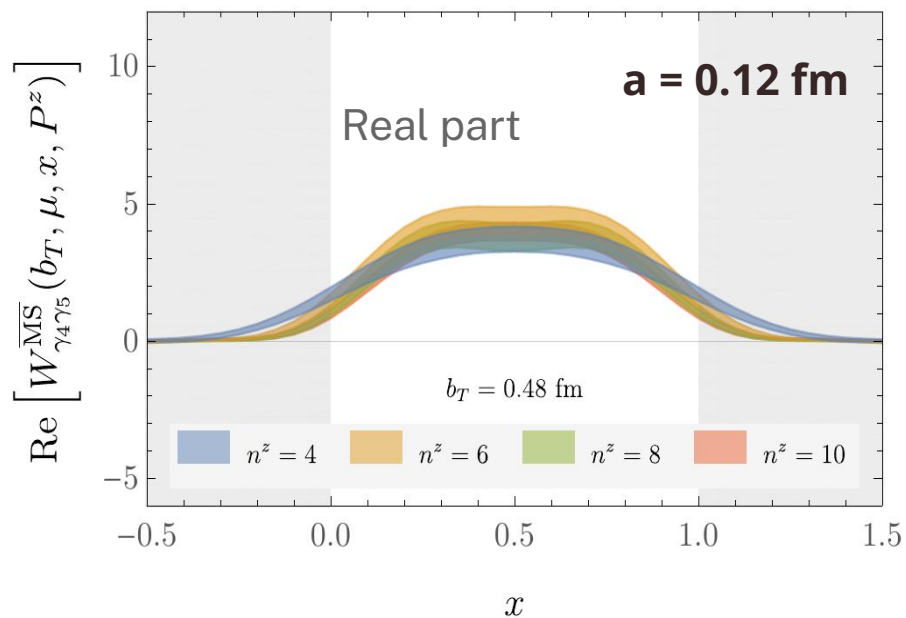


Position-space quasi-TMD WFs at 3 lattice spacings



Momentum-space quasi-TMDs

- Have support outside $x \in [0, 1]$, as expected.
- Converge to physical range $x \in [0, 1]$ with increasing $P^z = \frac{2\pi}{L}n^z$.



CS kernel estimate

$$\hat{\gamma}_{\Gamma}^{\overline{\text{MS}}}(b_T, x, P_1^z, P_2^z, \mu)$$

$$= \frac{1}{\ln(P_1^z/P_2^z)} \ln \left[\frac{W_{\Gamma}^{\overline{\text{MS}}}(b_T, x, P_1^z, \ell)}{W_{\Gamma}^{\overline{\text{MS}}}(b_T, x, P_2^z, \ell)} \right]$$

$$+ \delta\gamma_q^{\overline{\text{MS}}}(x, P_1^z, P_2^z, \mu)$$

- Separate for each momentum pair, b_T , Dirac / Γ , and matching.

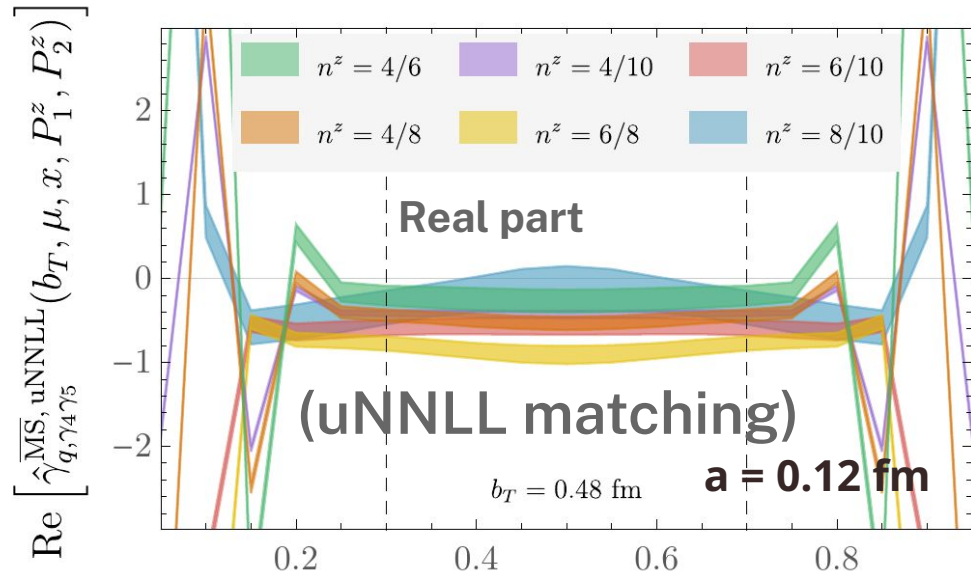
X. Ji et. al., Phys. Lett. B 811 [1911.03840]
 X. Ji and Y. Liu, PRD 105, [2106.05310]
 Z.-F. Deng et. al, JHEP 09, [2207.07280]

- Differ by power corrections:

$$\mathcal{O} \left(\frac{1}{(xP^z b_T)^2}, \frac{m_{\pi}^2}{(xP^z)^2} \right) + (x \leftrightarrow 1-x)$$

- Corrections $\sim P_1^z, \sim P_2^z$ partially cancel in ratios – **insufficient precision to fit & subtract power corrections**

- \Rightarrow Fit each estimator separately to a constant in $x \in [0.3, 0.7]$, then average fits at fixed b_T and matching accuracy.

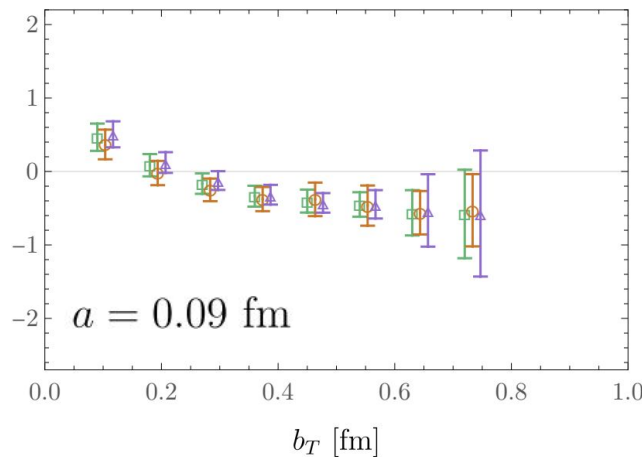
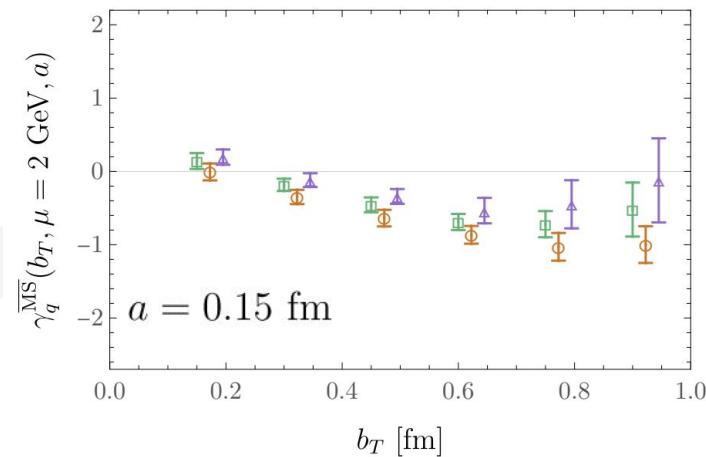
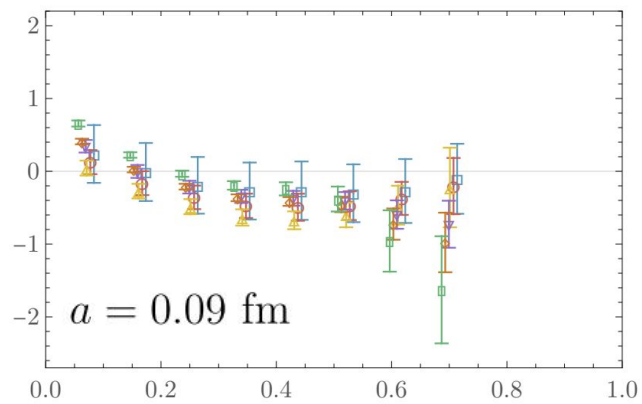
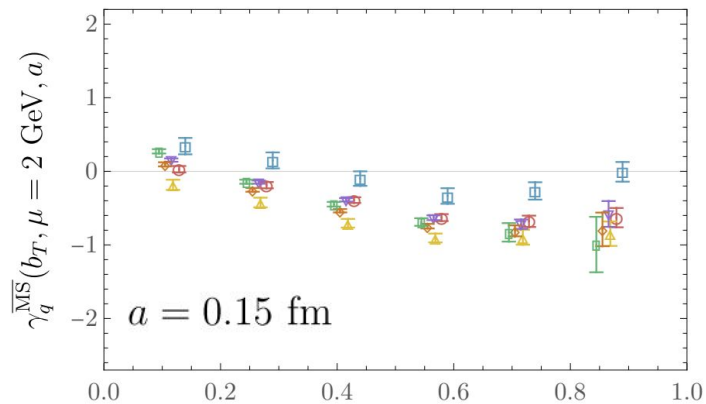


Weighted averages account for power corrections

Average over $P^z = \frac{2\pi}{N_z a} n^z$

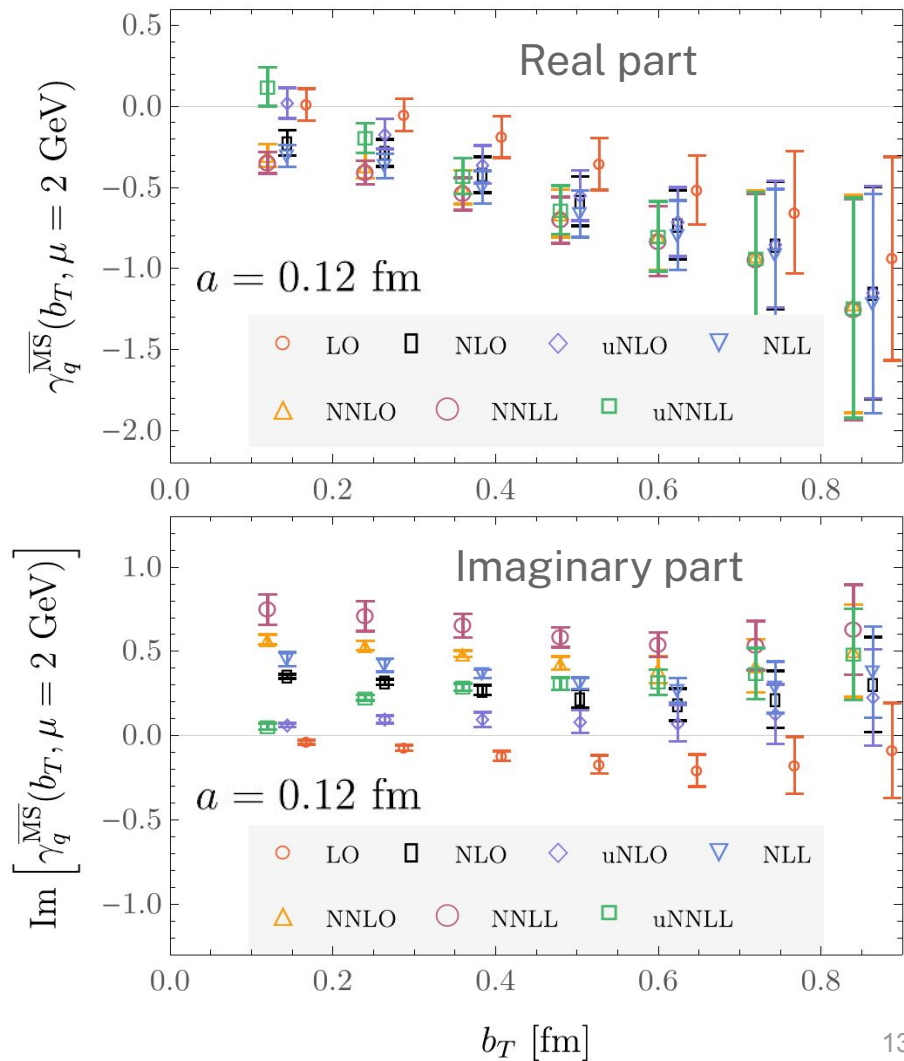


Average over Dirac (Γ) structures



Study of LaMET matching using **Re+Im** parts of CS kernel estimate

- The CS kernel is real-valued.
 - The CS kernel *estimate* has a **nonzero imaginary part** due to
 - poor perturbative convergence of matching coefficients
 - bT power corrections
- ⇒ **not treated as an independent systematic**
- M.-H. Chu et al. (LPC), PRD 106, 034509, [2204.00200]
 M.-H. Chu et al. (LPC), [2302.09961]
 M.-H. Chu et al. (LPC), [2306.06488]
- Re+Im parts used to characterize matching



Why bT-unexpanded matching

- Re part:** differs from expanded matching at small bT (beyond **LO**)

$\frac{1}{(xP^z b_T)^2}$ (Power corrections break down TMD factorization at small bT)

$$C_\phi(p^z, b_T, \mu) = C_\phi(p^z, \mu) + \delta C_\phi(p^z, b_T)$$

$p^z \in xP^z, \bar{x}P^z$

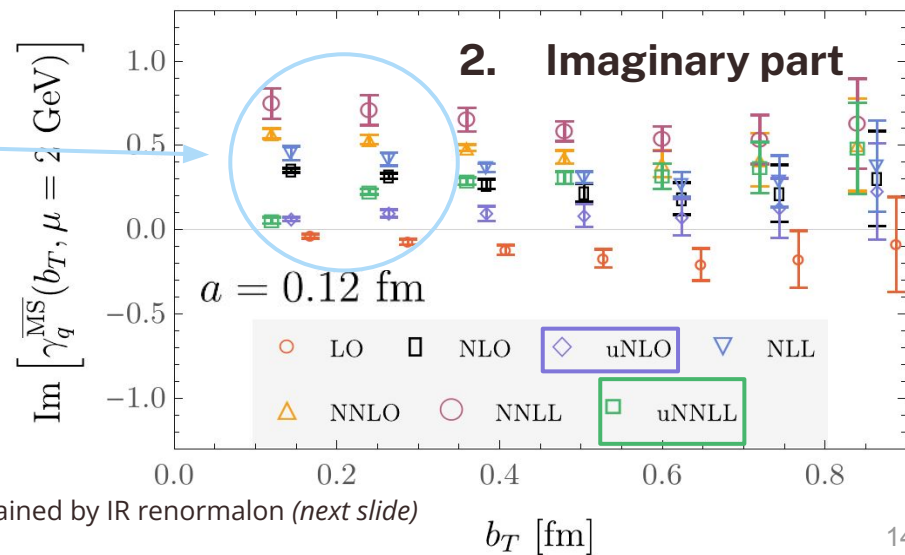
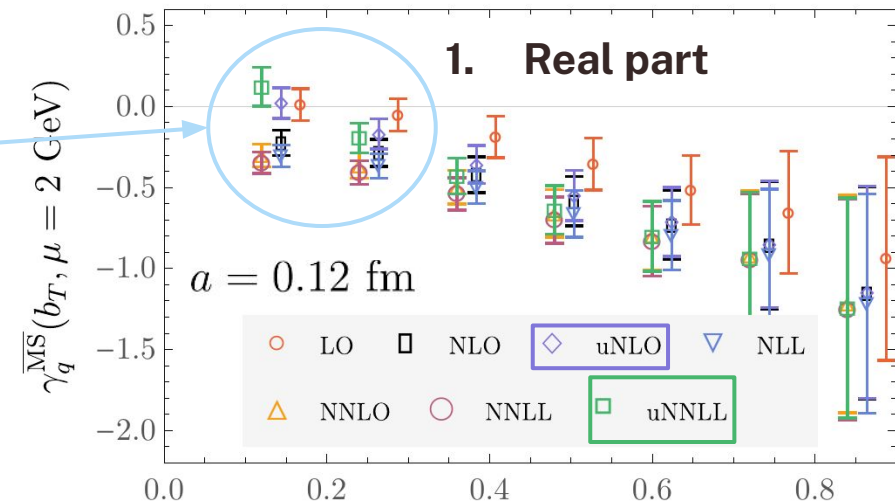
$\delta C_\phi(p^z, b_T)$ contains bT-dependent terms on $x \in (-\infty, \infty)$ suppressed in $P^z b_T$

2. Im part:

- Reduced by bT-unexpanded matching at small bT.
- Still nonzero at large bT:
 - even for **LO (= no matching)**
 - esp. for resummed logs (*LL)

However: no impact on the real part
 \Rightarrow no impact on CS kernel estimate

explained by IR renormalon (next slide)



Leading infrared renormalon

- Asymptotic series in matching coefficient

$$R(p^z, \mu) = i N_m \frac{\mu}{p^z} \sum_{n=0}^{\infty} \beta_0^n \alpha_s^{n+1}(\mu) n!$$

$= 0.552$ for 4 flavors
lowest-order β -function

$$p^z \in xP^z, \bar{x}P^z$$

- Leads to slow perturbative convergence in the imaginary part of CS kernel.

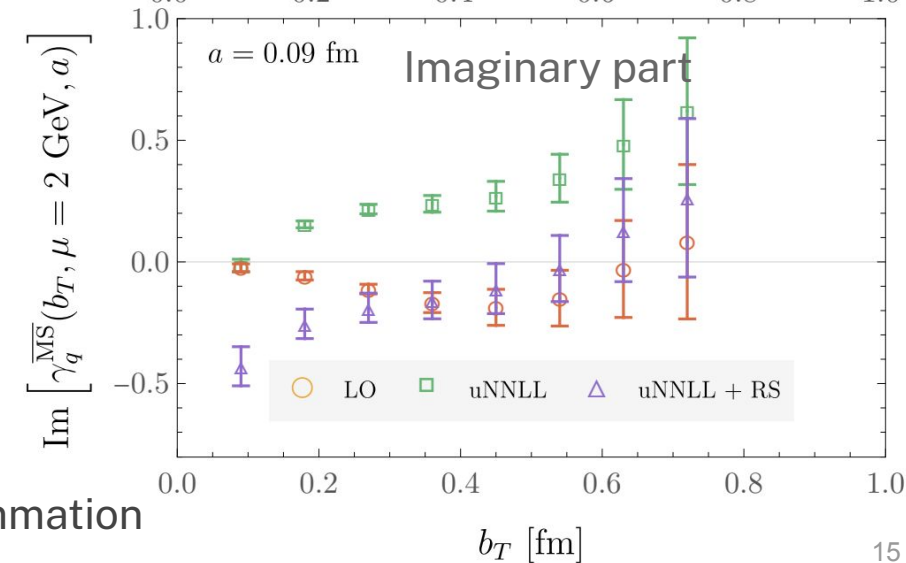
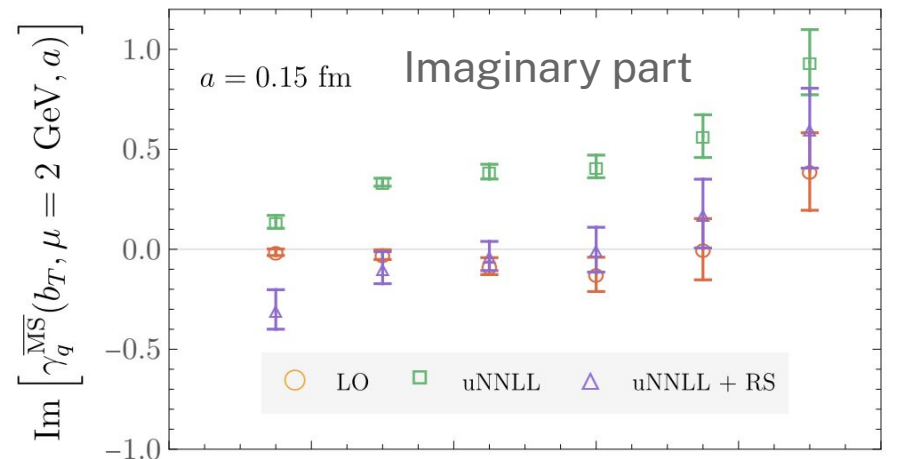
Y. Liu, Y. Su (LPC), JHEP02(204), [2311.06907]

- Leading renormalon resummation (LRR):**

$$C^{\text{LRR}}(p^z, \mu) = C(p^z, \mu) - R(p^z, \mu) + \mathcal{O}\left(\frac{\Lambda_{\text{QCD}}}{p^z}\right)$$

- Suppresses remaining p.c. at large b_T in the imaginary part for **uNNLL****
 - Not expected to work at small b_T (IR effect)
- \Rightarrow no unexplained systematics in **uNNLL**

Final determination: uNNLL = uNLO + resummation



CS kernel parameterization and continuum extrapolation

- Pheno params + **Discretization effects** modeled together:

$$\gamma_q^{\text{param.}}(b_T, \mu; B_{\text{NP}}, \{c_i\}, a)$$

$$= -2 \left[\mathcal{D}_{\text{pert.}}(b^*, \mu) + \mathcal{D}_{\text{NP}}(b_T, b^*; B_{\text{NP}}, \{c_i\}) \right] + k_1 \frac{a}{b_T} + k_2 \frac{a^2}{b_T^2}$$

$\xrightarrow{\text{best fit}} b_T b^* \left[c_0 + c_1 \ln \frac{b^*}{B_{\text{NP}}} \right]$

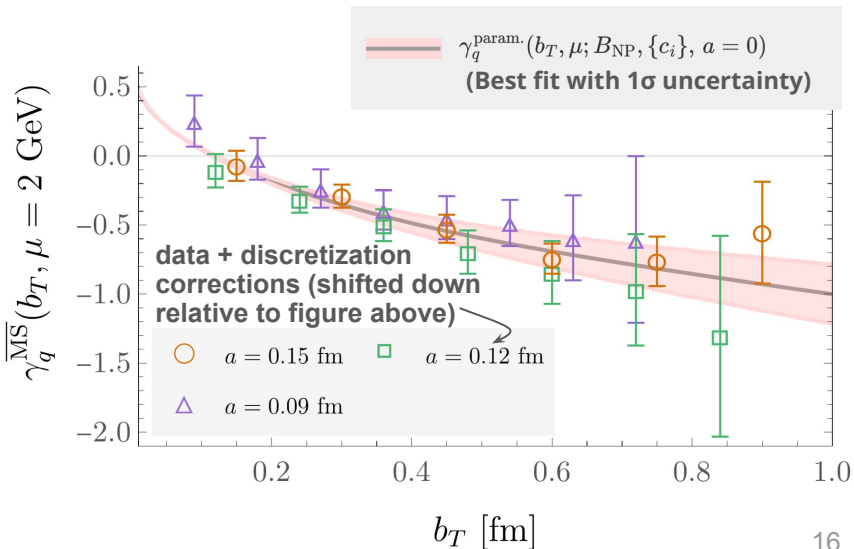
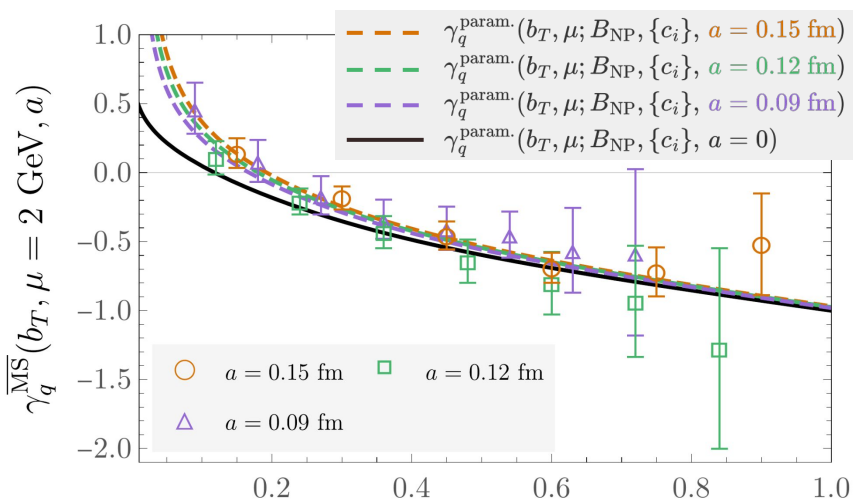
- Fits to different **NP models** consistent, directly comparable with **params** from pheno. results.

Discretization effects:

- ~**20%** from **best fit**:

- Fix subsets of params to **ref. values**
 - Optimize** others
 - Use AIC to pick **best fit**
(Akaike Information Criterion)
- $c_0 = 0.032(12),$
 $k_1 = 0.22(8),$
 $[c_1 = 0, B_{\text{NP}} = 2 \text{ GeV}]$
 $k_2 = 0]$

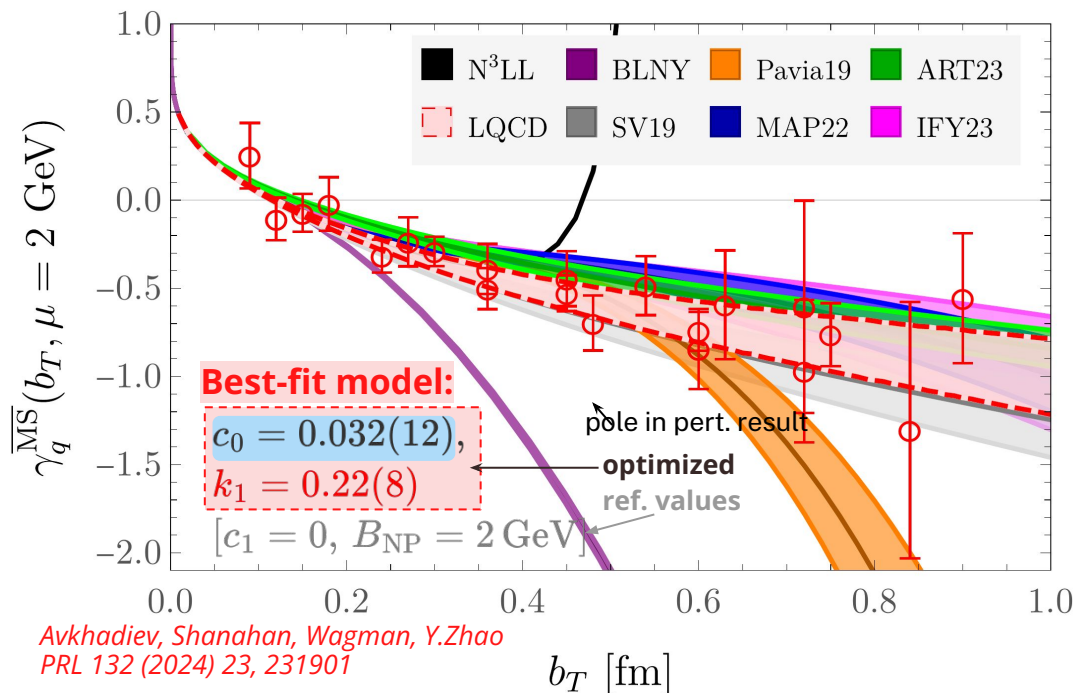
- ~**10-30%** range as **NP models** are varied



Summary and outlook

- **Systematic control** over quark mass, operator mixing, and discretization effects
- Sufficiently precise to **discriminate between some pheno models**
- Still not fitting power corrections, using weighted averages
- Improvements expected from
 - Coulomb Gauge fixing for stapleless calculations
 - **bT-dependent matching**, incl. in collinear factorization limit

Avkhadiev, Shanahan, Wagman, Y.Zhao
PRD 108 (2023) 11, 114505



Avkhadiev, Shanahan, Wagman, Y.Zhao
PRL 132 (2024) 23, 231901

X. Gao(Argonne), W-Y. Liu, Y. Zhao, PRD109 (2024) [2306.14960]

Y. Zhao [2311.01391]

Bollweg, X. Gao, Mukherjee, Y. Zhao, PLB 852 (2024) [2403.00664]

Talks: Tue Y. Zhao [9.20 am], X. Gao [9.50 am]

Wed Y.B. Yang [8.30 am], J. He [9.00 am]

Calculations of quark vs. gluon CS kernel differ by operator and matrix element, otherwise analogous

Quark CS kernel — completed

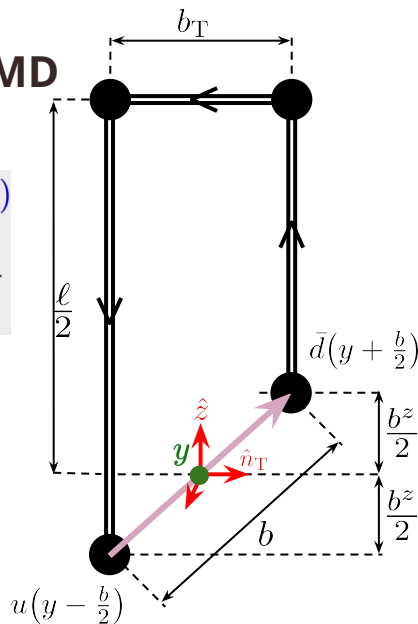
Computed using **quasi-TMD wavefunctions (WFs)**:

$$W_{\Gamma}(b_T, b^z, \ell, P^z) \quad (\Gamma \in \{\gamma^4, \gamma^5, \gamma^5\})$$

$$= \frac{\langle 0 | \mathcal{O}_{\Gamma}(b_T, b^z, \ell, P^z) | \pi(P^z) \rangle}{\langle 0 | \mathcal{O}_{\gamma^4, \gamma^5}(b_T, 0, \ell, 0) | \pi(0) \rangle}$$

$P_z=0, b_z=0$ matrix elt
to subtract divergences linear
in ℓ

Account for renormalization-
induced mixing between Γ
structures



Gluon CS kernel — ongoing

Computed using **quasi-TMD beam functions**:

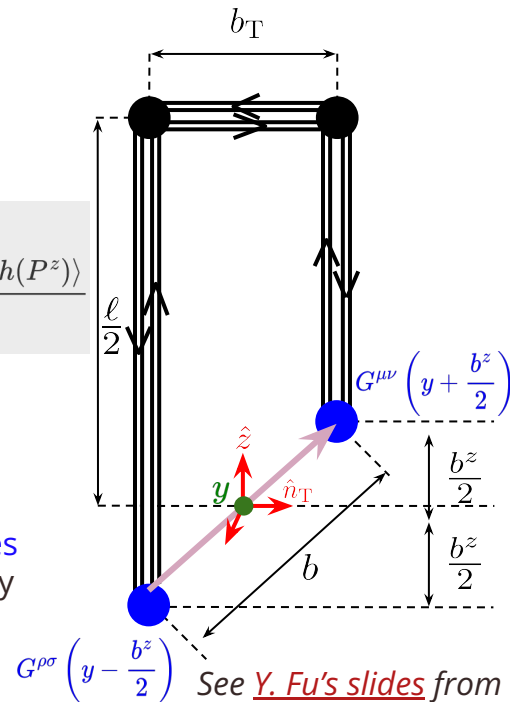
$$P^{\mu} P^{\nu} \tilde{B}_{g/h}^{\rho\sigma}(b^z, b_T, P^z, \ell)$$

$$= \frac{\langle h(P^z) | \mathcal{O}_g^{\mu\nu\rho\sigma}(b_T, b^z, 0, \ell) | h(P^z) \rangle}{\sqrt{Z_A(b_T, \ell)}}$$

Square root of adjoint
Wilson loop to subtract
divergences linear in ℓ

Can choose **Lorentz indices**
that lead to multiplicatively
renormalizable operators

J-H. Zhang, X. Ji,
Schäfer, W. Wang, S. Zhao,
PRL 122 (2019) [1808.10824]



See [Y. Fu's slides](#) from
Lattice 2024

Gluon calculation will require ~30x stats of the quark project

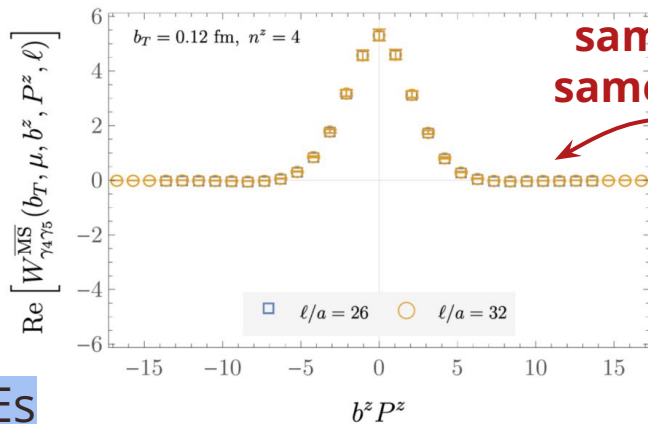
Position space MEs

- Quark ME has non-zero imaginary part
- Gluon ME real, and exactly bz-symmetric after averaging +/- bT

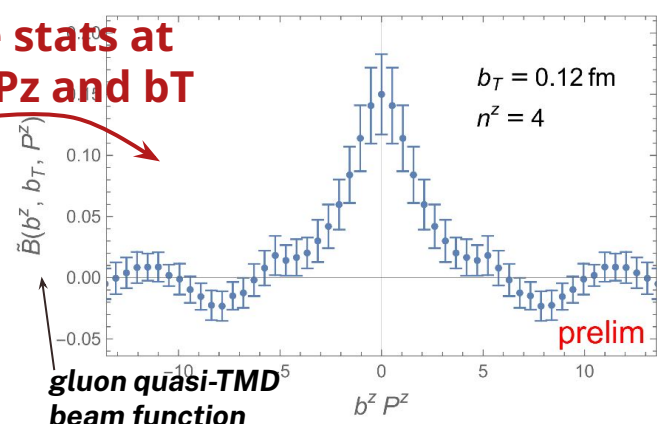
Fourier-transformed MEs

- Quark ME symmetric wrt $x \rightarrow 1-x$
- Gluon ME symmetric wrt $x \rightarrow -x$, **power corrections still most suppressed around $|x| \sim 0.5$**

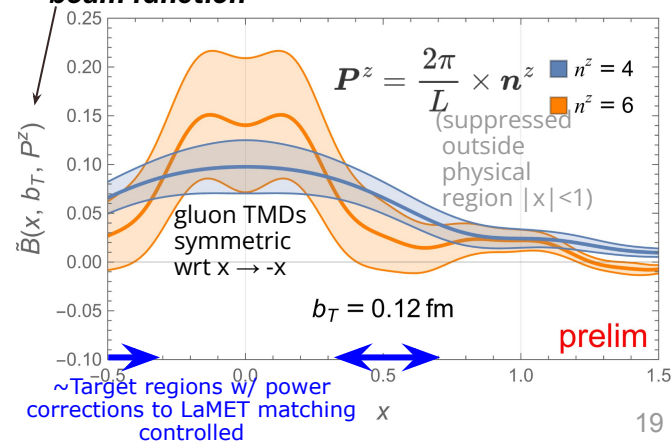
Quark CS kernel — completed



Gluon CS kernel — ongoing



gluon quasi-TMD⁵ beam function



Backup

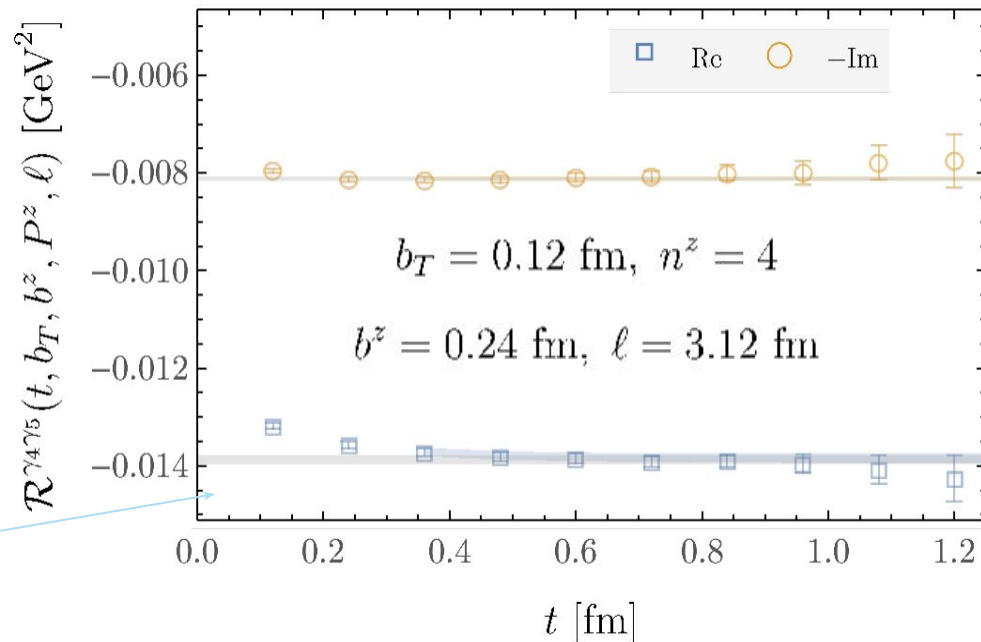
Unsubtracted quasi-TMD WFs: examples

- Extracted from correlation functions

$$\sum_{\mathbf{y}} e^{i\mathbf{P}\cdot\mathbf{y}} \left\langle \mathcal{O}_{\Gamma}(b_T, b^z, \mathbf{y}, \ell) \chi_{\mathbf{P}}^{\dagger}(0) \right\rangle$$

$$\xrightarrow{t \gg 0} \frac{Z_{\pi}^S(\mathbf{P})}{2E_{\pi}(\mathbf{P})} \tilde{\phi}_{\Gamma}(b_T, b^z, \mathbf{P}, \ell) e^{-E_{\pi}(\mathbf{P})t}$$

- Momentum-smeared interpolators $\chi_{\mathbf{P}}^{\dagger}$
- $E_{\pi}(\mathbf{P})$ and $Z_{\pi}^S(\mathbf{P})$ fit and cancelled in ratios $\mathcal{R}^{\Gamma}(t, b_T, b^z, P^z, \ell)$:
- Plateau gives $\tilde{\phi}_{\Gamma}(b_T, b^z, \mathbf{P}, \ell)$.
- Repeated for each P^z, b_T, b^z, ℓ .

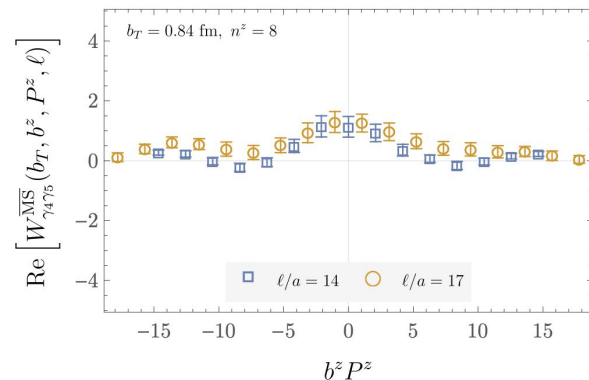
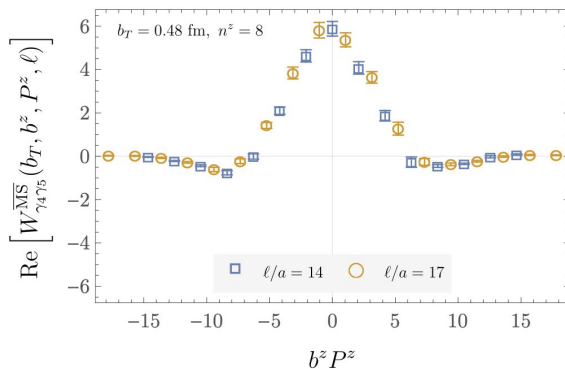
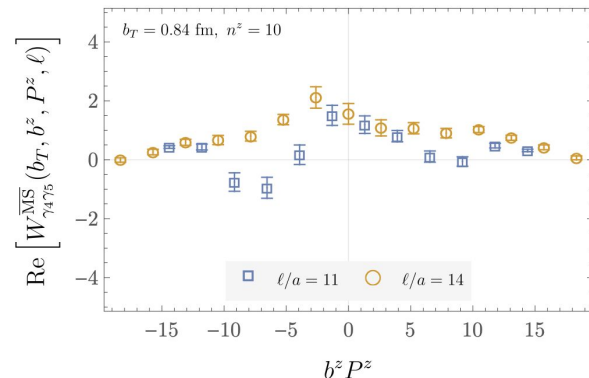
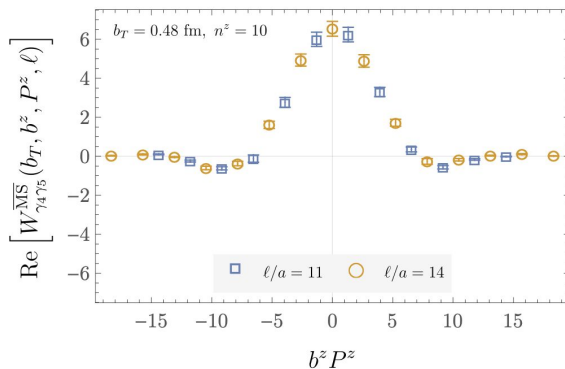


- A range of time windows chosen systematically
- Covariance matrix from bootstrap + linear shrinkage
- Correlated determinations between staple geometries
- AIC-preferred fits (1 + 2 state)
- Further selection cuts + combine in weighted average

TMD WFs in position space

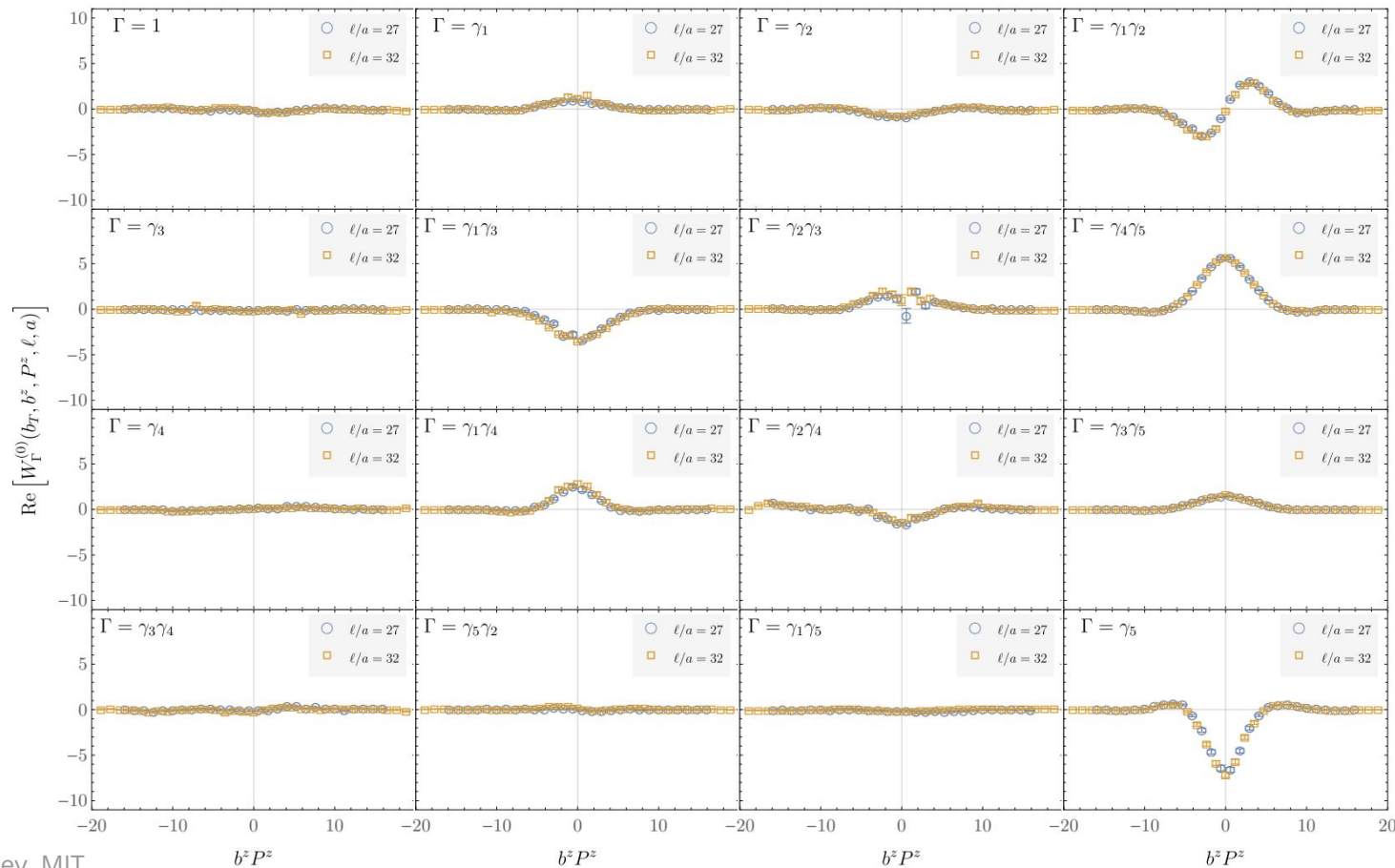
Statistical noise makes computation challenging for large P^z , ℓ , and b_T

- $b_T = 0.48$ fm, 0.84 fm
left to right
- $P^z = 2.15$ GeV, 1.72 GeV
top to bottom
- Our group's previous calculation had
 $b_T^{\max} = 0.48$ fm,
 $P_{\max}^z = 1.51$ GeV



MEs with all 16 Dirac structures calculated

$a = 0.09 \text{ fm}, b_T = 0.36 \text{ fm}, P^z = 1.3 \text{ GeV}$



Mixing effects quantified with RIxMOM

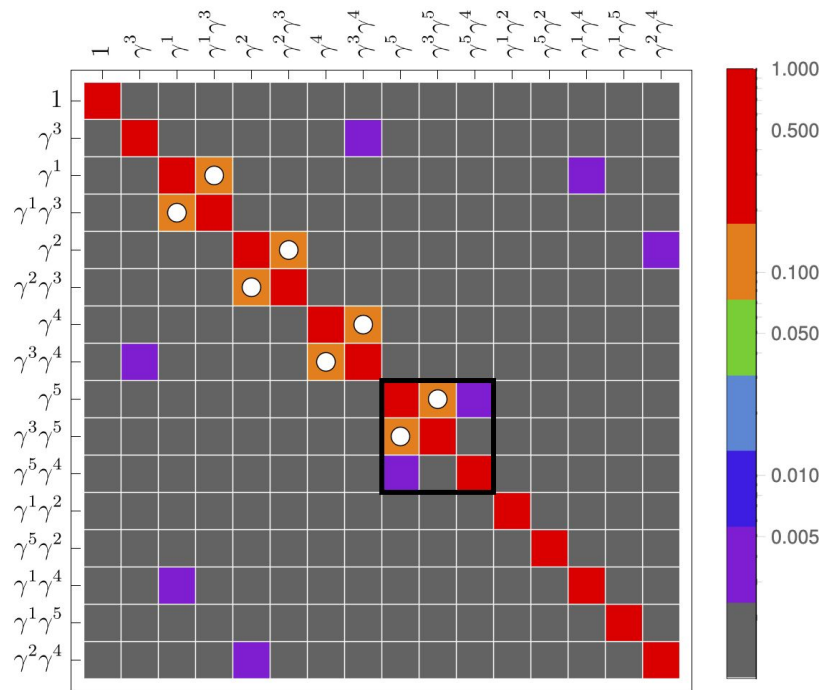
- Calculation of mixing effects in RIxMOM independent of staple geometry.

$$W_{\Gamma}^{\overline{\text{MS}}}(b_T, \mu, b^z, P^z, \ell) = \sum_{\Gamma'} Z_{\Gamma\Gamma'}^{\overline{\text{MS}}}(\mu) W_{\Gamma'}^{(0)}(b_T, b^z, P^z, \ell)$$

- Full 16x16 mixing matrix computed

$$\mathcal{M}_{\Gamma\Gamma'}^{\text{RI/xMOM}}(p_R, \xi_R, a) \equiv \frac{\text{Abs}[Z_{\Gamma\Gamma'}^{\text{RI/xMOM}}(p_R, \xi_R, a)]}{\frac{1}{16} \sum_{\Gamma} \text{Abs}[Z_{\Gamma\Gamma}^{\text{RI/xMOM}}(p_R, \xi_R, a)]}$$

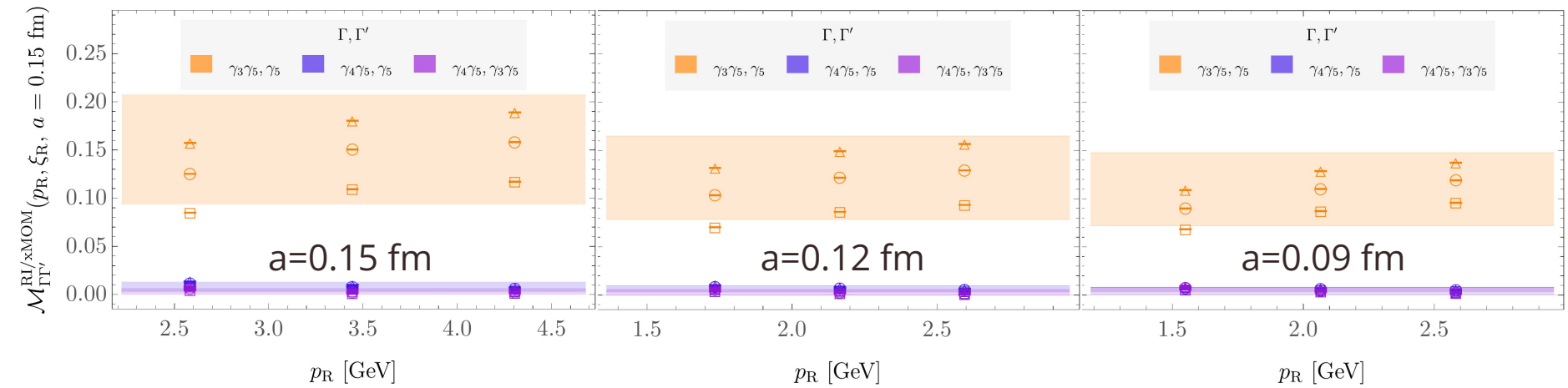
- Dominant mixings consistent with lattice perturbation theory at 1-loop.*



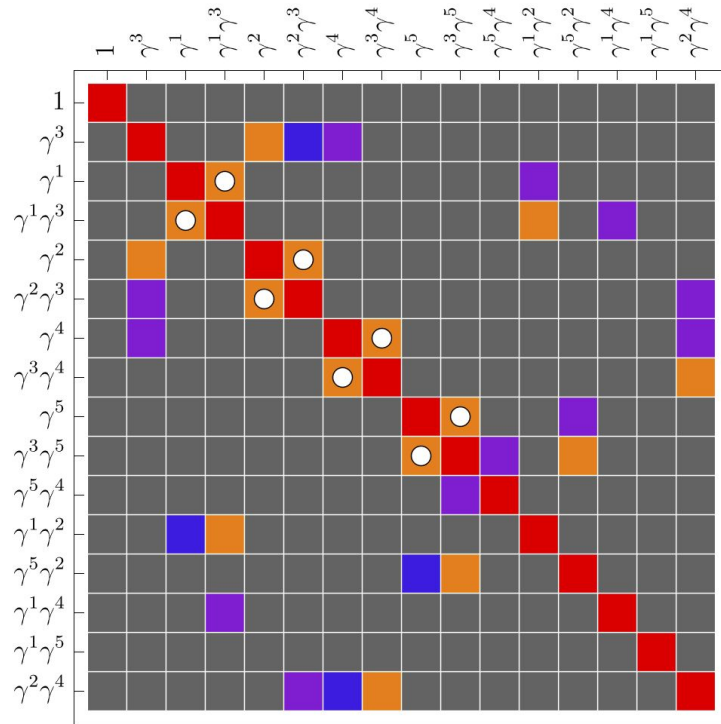
$$p_R^\mu = \frac{2\pi}{L} \times (0, 0, 10, 0), \quad \xi = 0.24 \text{ fm}$$

X. Ji, et. al, PRL 120 (2018), [1706.08962] *M. Constantinou et al., PRD 99 (2019), [1901.03862]
 J. Green et. al, PRL 121 (2018), [1707.07152] Y. Ji et. al., PRD 104 (2021), [2104.13345]
 J. Green et. al, PRD 101 (2020), [2002.09408] C. Alexandrou et al., [2305.11824]

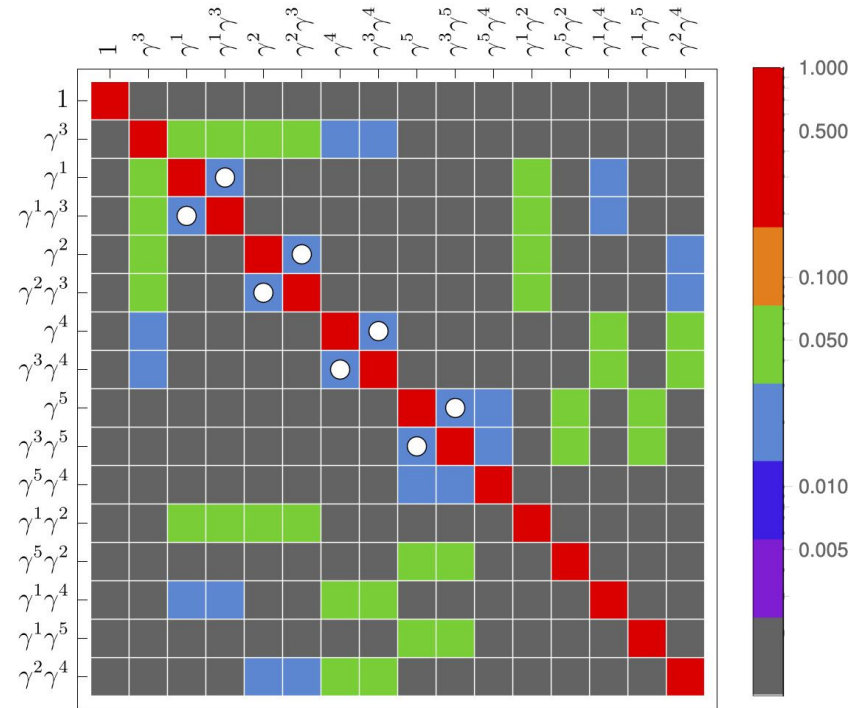
Mixing reduced at finer lattice spacings, as expected



Scheme dependence of mixing patterns



$$p_R^\mu = \frac{2\pi}{L} \times (0, 10, 0, 0), \xi = 0.24 \text{ fm}$$



$$p_R^\mu = \frac{2\pi}{L} \times (6, 6, 6, 6), \xi = 0.24 \text{ fm}$$

TMD WFs in momentum space

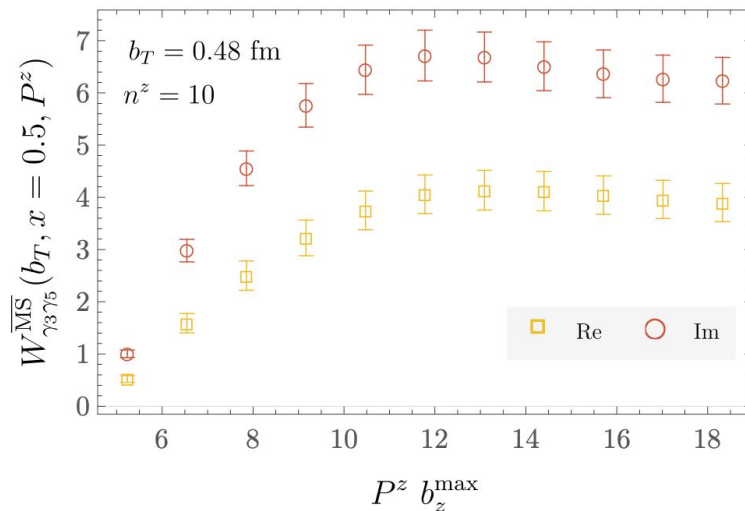
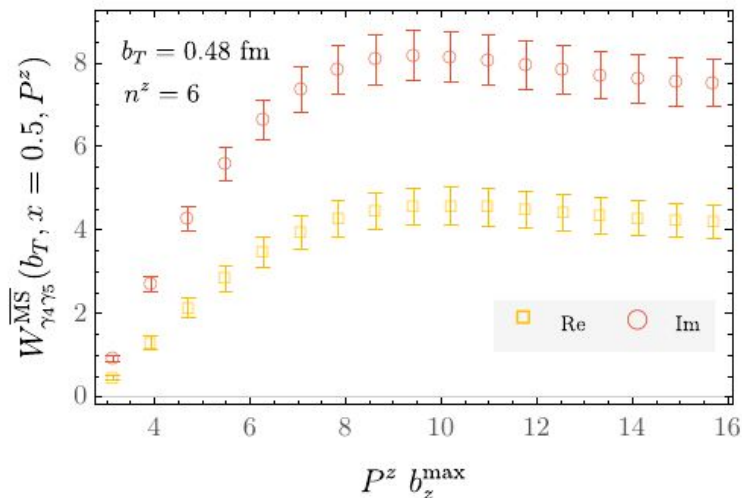
$$\gamma_q(\mu, b_T) = \lim_{a \rightarrow 0} \frac{1}{\ln(P_1^z/P_2^z)} \ln \left[\frac{\int db^z e^{ib^z x P_1^z} P_1^z \sum_{\Gamma'} Z_{\Gamma'}(\mu, a) \lim_{\ell \rightarrow \infty} W_O^{\Gamma'}(b^z, b_T, \ell, P_1^z, a)}{\int db^z e^{ib^z x P_2^z} P_2^z \sum_{\Gamma'} Z_{\Gamma'}(\mu, a) \lim_{\ell \rightarrow \infty} W_O^{\Gamma'}(b^z, b_T, \ell, P_2^z, a)} \right] + \delta\gamma_q(\mu, b_T, P_1^z, P_2^z) + \mathcal{O}\left(\frac{1}{(xP^z b_T)^2}, \frac{M^2}{(xP^z)^2}, \frac{\Lambda_{\text{QCD}}^2}{(xP^z)^2}\right)$$

bz range sufficient to use a Discrete Fourier Transform

$$\bar{W}_{\Gamma}^{\overline{\text{MS}}}(b_T, \mu, x, P^z) = \frac{P^z}{2\pi} N_{\Gamma}(P) \sum_{|b_z| \leq b_z^{\max}} e^{i(x-\frac{1}{2})P^z b^z} \bar{W}_{\Gamma}^{\overline{\text{MS}}}(b_T, \mu, b^z, P^z)$$

Normalization factor to compare between Dirac structures

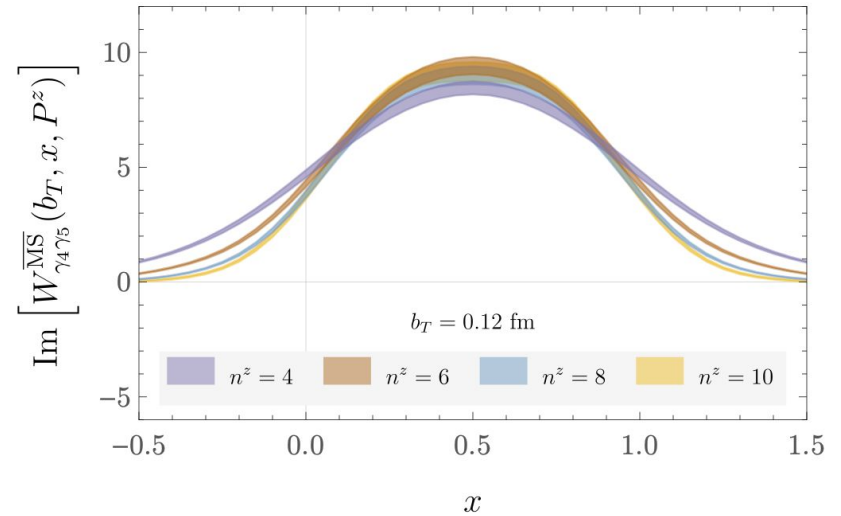
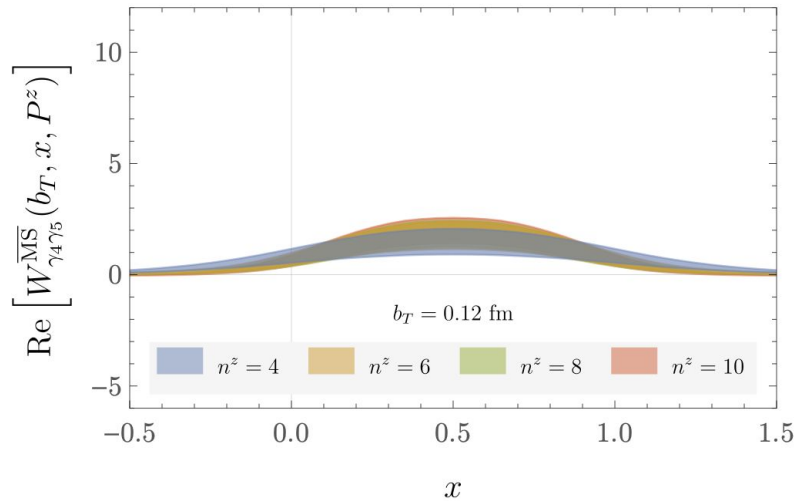
The DFT is stable to decreasing the range in b_T^{\max} :



TMD WFs in momentum space

$$\gamma_q(\mu, b_T) = \lim_{a \rightarrow 0} \frac{1}{\ln(P_1^z/P_2^z)} \ln \left[\frac{\int db^z e^{ib^z x P_1^z} P_1^z \sum_{\Gamma'} Z_{\Gamma'}(\mu, a) \lim_{\ell \rightarrow \infty} W_O^{\Gamma'}(b^z, b_T, \ell, P_1^z, a)}{\int db^z e^{ib^z x P_2^z} P_2^z \sum_{\Gamma'} Z_{\Gamma'}(\mu, a) \lim_{\ell \rightarrow \infty} W_O^{\Gamma'}(b^z, b_T, \ell, P_2^z, a)} \right] + \delta\gamma_q(\mu, b_T, P_1^z, P_2^z) + \mathcal{O}\left(\frac{1}{(xP^z b_T)^2}, \frac{M^2}{(xP^z)^2}, \frac{\Lambda_{\text{QCD}}^2}{(xP^z)^2}\right)$$

See convergence to the physical range $x \in [0, 1]$ with increasing $P^z = \frac{2\pi}{L} n^z$

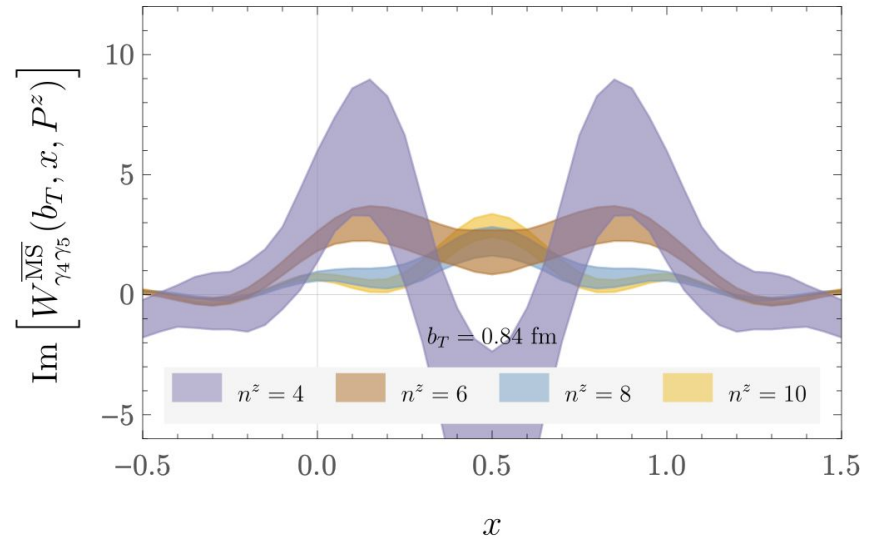
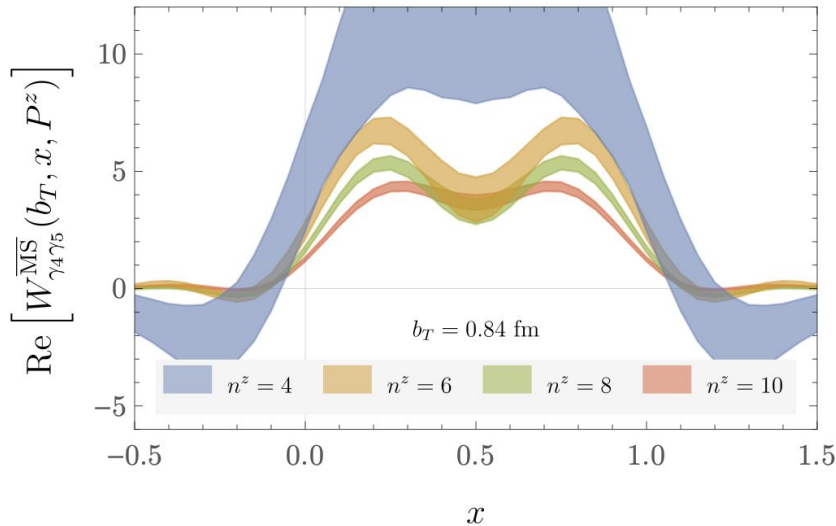


TMD WFs in momentum space

$$\gamma_q(\mu, b_T) = \lim_{a \rightarrow 0} \frac{1}{\ln(P_1^z/P_2^z)} \ln \left[\frac{\int db^z e^{ib^z x P_1^z} P_1^z \sum_{\Gamma'} Z_{\Gamma'}(\mu, a) \lim_{\ell \rightarrow \infty} W_{\mathcal{O}}^{\Gamma'}(b^z, b_T, \ell, P_1^z, a)}{\int db^z e^{ib^z x P_2^z} P_2^z \sum_{\Gamma'} Z_{\Gamma'}(\mu, a) \lim_{\ell \rightarrow \infty} W_{\mathcal{O}}^{\Gamma'}(b^z, b_T, \ell, P_2^z, a)} \right]$$

$$+ \delta\gamma_q(\mu, b_T, P_1^z, P_2^z) + \mathcal{O}\left(\frac{1}{(xP^z b_T)^2}, \frac{M^2}{(xP^z)^2}, \frac{\Lambda_{\text{QCD}}^2}{(xP^z)^2}\right)$$

See convergence to the physical range $x \in [0, 1]$ with increasing $P^z = \frac{2\pi}{L} n^z$



NLO, NNLO, and resummations

The correction is given by coefficients

$$\delta\gamma_q(x, P_1^z, P_2^z, \mu) \equiv \frac{1}{\ln(P_1^z/P_2^z)} \left(\ln \frac{C_\phi(xP_2^z, \mu)}{C_\phi(xP_1^z, \mu)} + (x \leftrightarrow \bar{x}) \right)$$

$C_\phi(p^z, \mu)$ appear in the TMD WF matching formula and are computed perturbatively as

$$C_\phi(p^z, \mu) = 1 + \sum_{n=1} \left(\frac{\alpha_s(\mu)}{4\pi} \right)^n C_\phi^{(n)}(p^z, \mu)$$

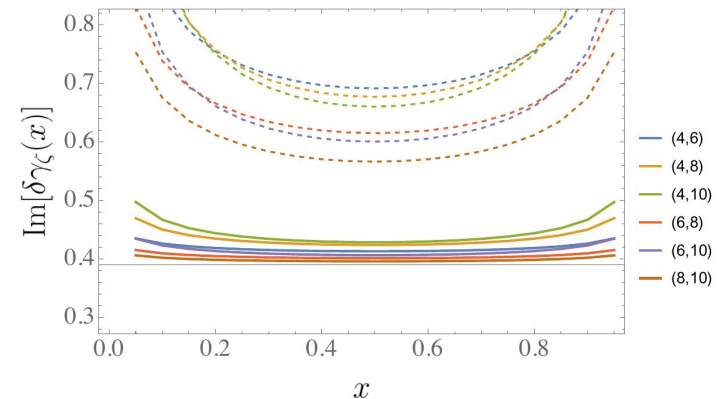
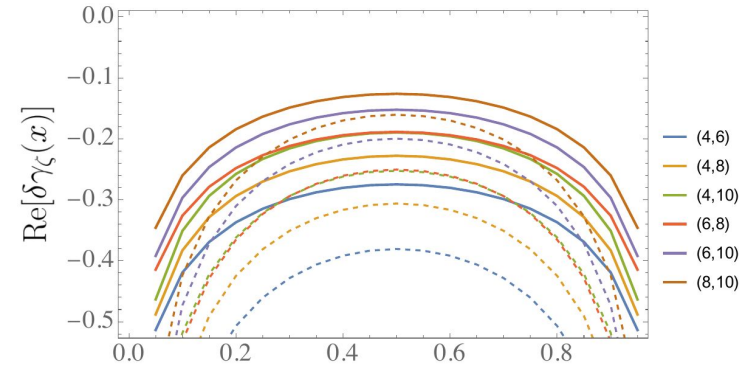
at LO, NLO and recently at NNLO, and resummed as

O. del Río and A. Vladimirov, [2304.14440]

X. Ji et. al, [2305.04416]

$$C_\phi(p^z, \mu) = C_\phi(p^z, 2p^z) \times \exp[K_\phi(p^z, 2p^z)]$$

Resummation kernel



NLO (solid) and NNLO (dashed);
No convergence in the imaginary part

NLL and NNLL

X. Ji et. al., Phys. Lett. B 811 [1911.03840]
 Ebert et. al, JHEP 04 (2022), [2201.08401]

Resummation kernel is $K_\phi(2p^z, \mu) = 2K_\Gamma(2p^z, \mu) - K_{\gamma_\mu}(2p^z, \mu) - i\pi\eta(2p^z, \mu)$

$$K_{\gamma_\mu}(\mu_0, \mu) = \int_{\alpha_s(\mu_0)}^{\alpha_s(\mu)} \frac{d\alpha_s}{\beta(\alpha_s)} \gamma_\mu(\alpha_s),$$

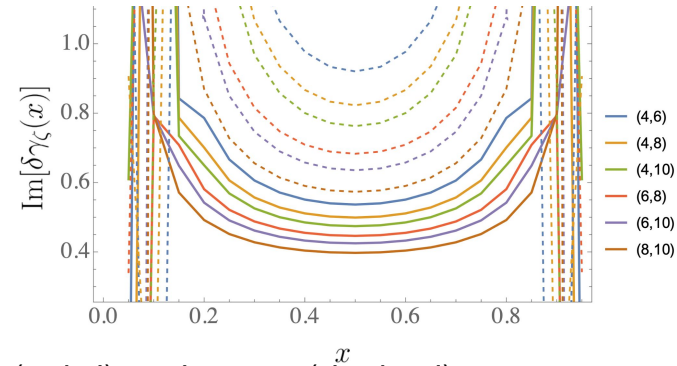
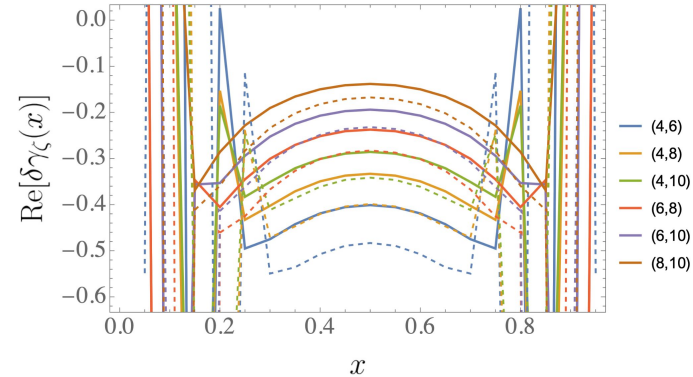
$$K_\Gamma(\mu_0, \mu) = \int_{\alpha_s(\mu_0)}^{\alpha_s(\mu)} \frac{d\alpha_s}{\beta(\alpha_s)} \Gamma_{\text{cusp}}(\alpha_s) \int_{\alpha_s(\mu_0)}^{\alpha_s} \frac{d\alpha'_s}{\beta(\alpha'_s)},$$

$$\eta_\Gamma(\mu_0, \mu) = \int_{\alpha_s(\mu_0)}^{\alpha_s(\mu)} \frac{d\alpha_s}{\beta(\alpha_s)} \Gamma_{\text{cusp}}(\alpha_s)$$

where $\Gamma_{\text{cusp}}(\alpha_s(\mu)) = \frac{d\gamma_\mu(p^z, \mu)}{d \ln p^z}$ and $\gamma_\mu(p^z, \mu) \equiv \frac{d \ln C_\phi(p^z, \mu)}{d \ln \mu}$

are computed perturbatively at following loop orders for each resummation accuracy:

| | K_Γ | K_{γ_C} | K_{γ_μ} | η | C_ϕ |
|------|------------|----------------|------------------|--------|----------|
| NLL | 2 | 1 | 1 | 1 | 0 |
| NNLL | 3 | 2 | 2 | 2 | 1 |



NLL (solid) and NNLL (dashed)
No convergence in the imaginary part

bT-dependent matching

Matching coefficients C include are a $P^z b_T \gg 1$ limit of

$$\mathbf{C}_\phi(p^z, b_T, \mu) = C_\phi(p^z, \mu) + \delta C_\phi(p^z, b_T)$$

uNLO

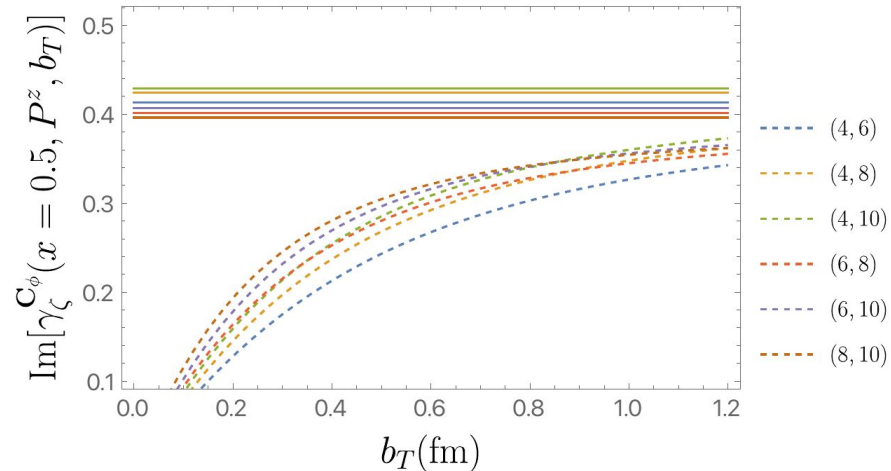
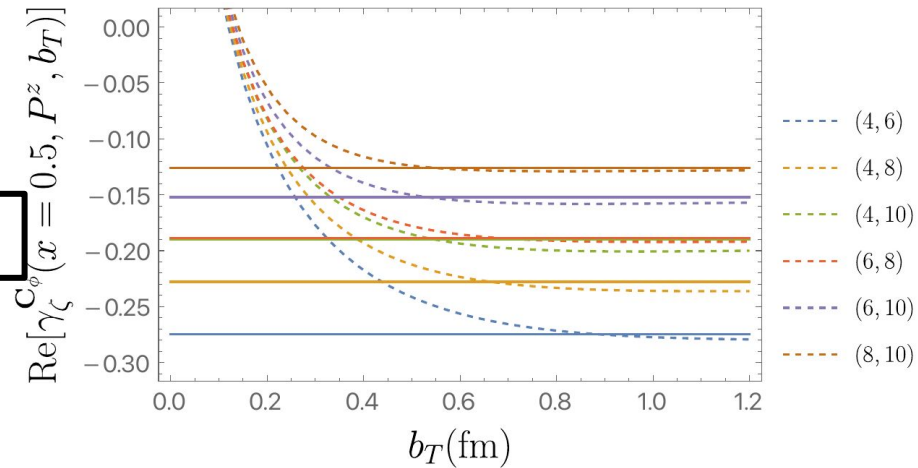
$$p^z \in xP^z, \bar{x}P^z$$

- $\delta C_\phi(p^z, b_T)$ contains bT-dependent terms on $x \in (-\infty, \infty)$ suppressed in $P^z b_T$

- Has been computed at NLO.
- Corresponding unexpanded (in bT) matching correction reveals power corrections in $1/Pz$ bT.
- Imaginary part more sensitive to power corrections => not taken as a systematic uncertainty directly.

M. A. Ebert et. al., JHEP 09, 037, [1901.03685]
Z.-F. Deng et. al, JHEP 09, [2207.07280]

M.-H. Chu et al. (LPC), PRD 106, 034509, [2204.00200]
M.-H. Chu et al. (LPC), [2302.09961]
M.-H. Chu et al. (LPC), [2306.06488]

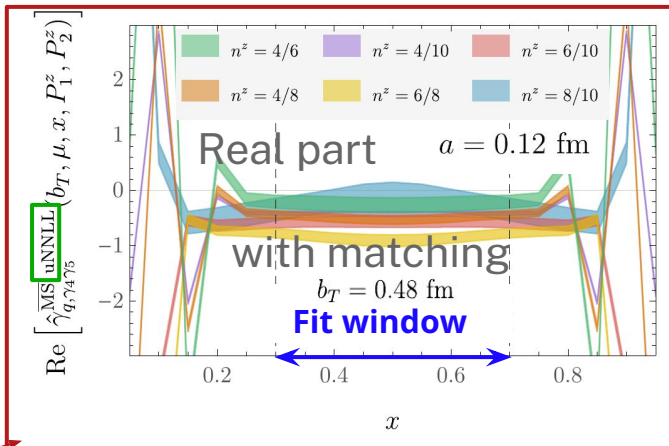


Dashed: **uNLO**, solid: NLO.

Power corrections expected to decrease with higher-order **LaMET** matching

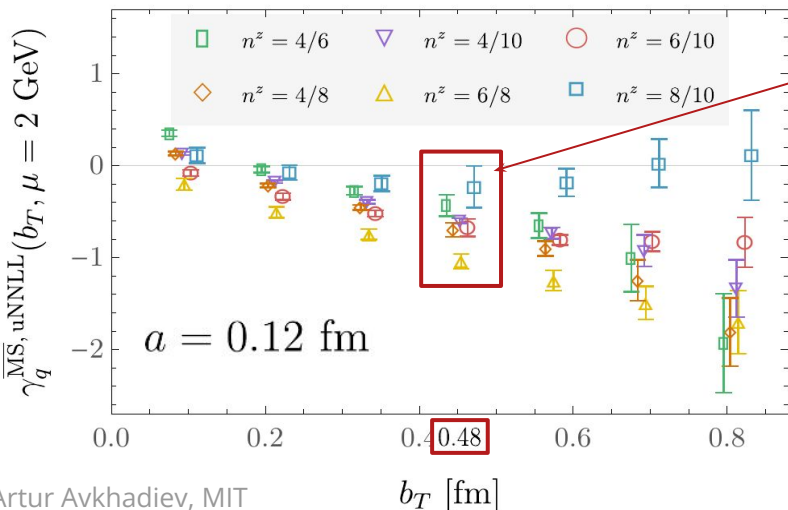
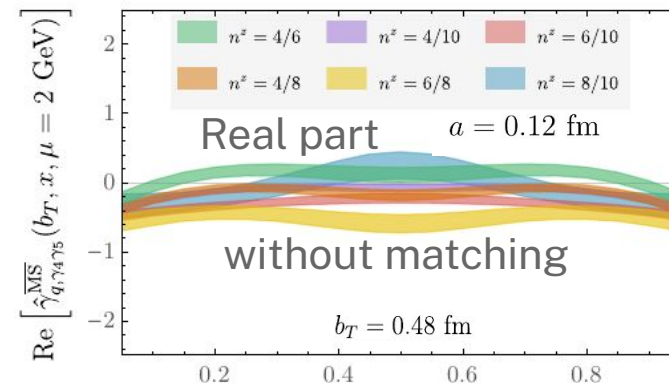
$$\gamma_q(b_T, \mu) = \lim_{\ell \rightarrow \infty} \frac{1}{\ln(P_1^z/P_2^z)} \times \ln \left[\frac{\int db^z e^{ib^z(x-\frac{1}{2})P_1^z} N_{\Gamma} \sum_{\Gamma} Z_{\Gamma}(b^z, b_T, \ell, P_1^z)} \lim_{\ell \rightarrow \infty} W_{\Gamma}(b^z, b_T, \ell, P_1^z)}{\int db^z e^{ib^z(x-\frac{1}{2})P_2^z} N_{\Gamma} \sum_{\Gamma} Z_{\Gamma}(b^z, b_T, \ell, P_2^z)} \lim_{\ell \rightarrow \infty} W_{\Gamma}(b^z, b_T, \ell, P_2^z)} \right] + \delta\gamma_q(\mu, P_1^z, P_2^z) + \mathcal{O}(a) \text{ p.d.c.}$$

- **Matching applied before weighted averaging** to ratios of MEs for each b_T, P_z pair, Dirac (Γ) structure, and a
- Final results use b_T -unexpanded, next-to-next-to-leading log (**uNNLL**) matching **with leading renormalon subtraction**

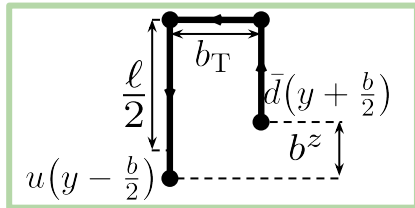


Fit each band separately to a constant in $x \in [0.3, 0.7]$ to get points at fixed b_T (**power corrections enhanced at $x \sim 0$ and $x \sim 1$**)

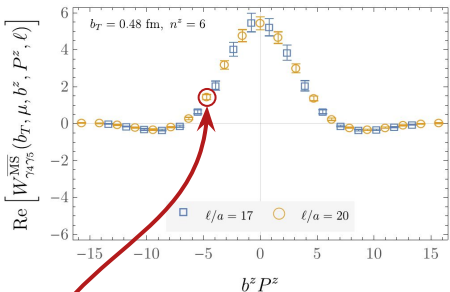
$$\mathcal{O}\left(\frac{\Lambda_{\text{QCD}}}{xP^z}, \frac{1}{b_T(xP^z)}\right) + (x \leftrightarrow 1-x)$$



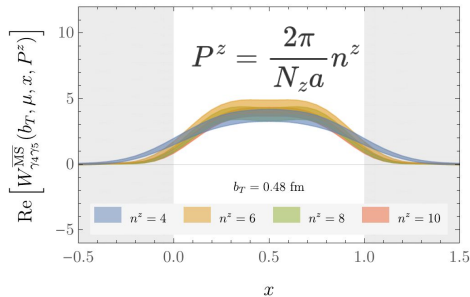
Rest of LQCD analysis remains as before – now w/ calculations at 2 additional lattice spacings



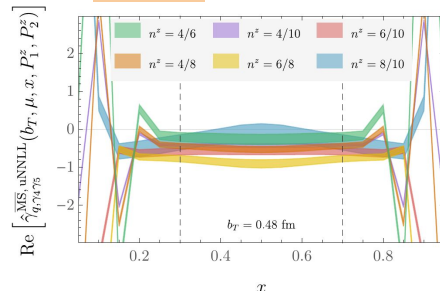
Calculate position-space MEs



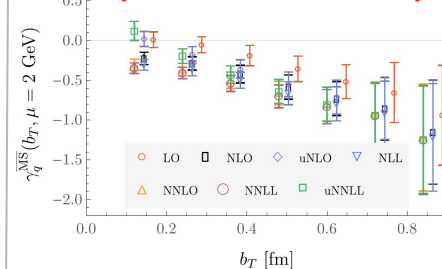
Fourier transform (FT) to momentum-space MEs



Form ratios of MEs + match + fit in x



...repeat for each b_T (... and for each a)



$$\sum_{\Gamma'} Z_{\Gamma\Gamma'}(\mu) \lim_{\ell \rightarrow \infty} W_O^{\Gamma'}(b^z, b_T, \ell, P_1^z)$$

$$W_{\Gamma}(b_T, b^z, \ell, P^z)_{\Gamma \in \{\gamma^4, \gamma^5, \gamma^5\}} = \frac{\langle 0 | \mathcal{O}_{\Gamma}(b_T, b^z, \ell, P^z) | \pi(P^z) \rangle}{\langle 0 | \mathcal{O}_{\gamma^4, \gamma^5}(b_T, 0, \ell, 0) | \pi(0) \rangle}$$

$$\int db^z e^{ib^z x P_1^z} P_1^z N_{\Gamma}(P_1^z)$$

$$\sum_{\Gamma'} Z_{\Gamma\Gamma'}(\mu) \lim_{\ell \rightarrow \infty} W_O^{\Gamma'}(b^z, b_T, \ell, P_1^z)$$

$$\gamma_q(b_T, \mu) = \lim_{a \rightarrow 0} \frac{1}{\ln(P_1^z/P_2^z)} \ln \left[\frac{\int db^z e^{ib^z x P_1^z} P_1^z N_{\Gamma}(P_1^z)}{\int db^z e^{ib^z x P_2^z} P_2^z N_{\Gamma}(P_2^z)} \right] \sum_{\Gamma'} Z_{\Gamma\Gamma'}(\mu) \lim_{\ell \rightarrow \infty} W_O^{\Gamma'}(b^z, b_T, \ell, P_1^z) + \delta\gamma_q(\mu, P_1^z, P_2^z) + \text{p.c.}$$

Each plotted point is a separate ME calculation (defined by b^z , P^z , b_T , ℓ , and Dirac (Γ) structure).

Discrete FT needs sufficient range in $b^z P^z$ to avoid truncation effects in x space (each P^z , b_T , Γ)

Needs careful choices of:

- P^z : several pairs to characterize **p.c.**, large enough (**p.c.**), small enough (disc. effects, stat. noise).
- b_T : large enough to see NP region, small enough to manage stat. noise.

Summary and Outlook

Quark CS kernel — completed

- **Systematic control** over quark mass, operator mixing, and discretization effects
- Sufficiently precise to **discriminate between some pheno models** from global analyses
- Still not fitting power corrections, using weighted averages
- Improvements expected from Coulomb Gauge fixing, b_T -dependent matching

Glue CS kernel — ongoing

- Need **~30x more stats** than in quark project
- No global analysis results yet, but expected with EIC data — **lattice QCD + LaMET will provide a prediction**

